POWER ELECTRONICS EUROPE

ISSUE 1 – Feb/March 2021 www.power-mag.com

POWER SEMICONDUCTORS

New Developments in RET Technology

Also inside this issue

Opinion | Research
Market News | Industry News
Website Locator

THE EUROPEAN JOURNAL FOR POWER ELECTRONICS AND TECHNOLOGY

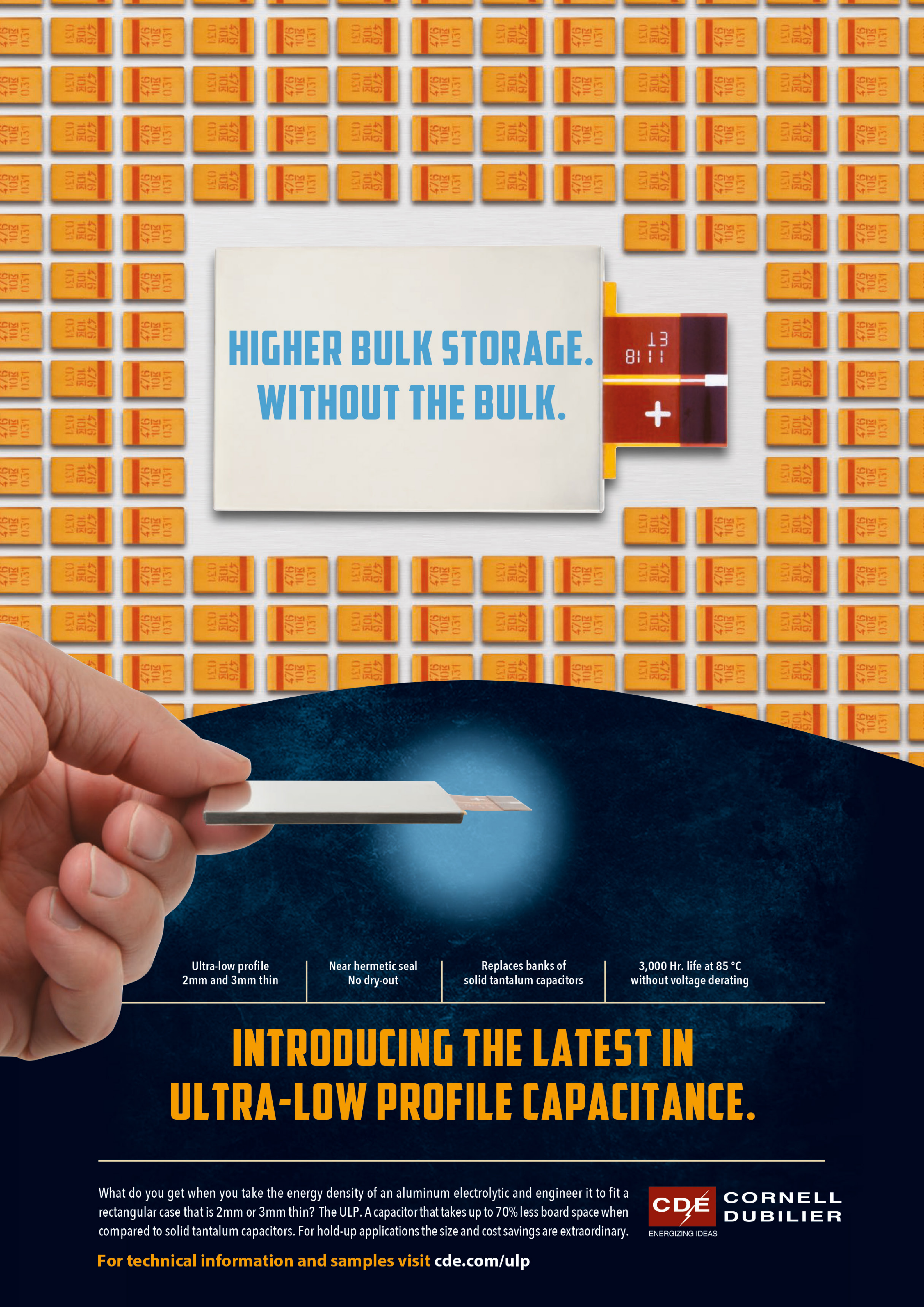
HIGHER BULK STORAGE.
WITHOUT THE BULK.
Ultra-low profile
2mm and 3mm thin
Near hermetic seal
No dry-out
Replaces banks of
solid tantalum capacitors
3,000 Hr. life at 85 °C
without voltage derating
INTRODUCING THE LATEST IN
ULTRA-LOW PROFILE CAPACITANCE.
What do you get when you take the energy density of an aluminum electrolytic and engineer it to fit a rectangular case that is 2mm or 3mm thin? The ULP. A capacitor that takes up to 70% less board space when compared to solid tantalum capacitors. For hold-up applications the size and cost savings are extraordinary.
For technical information and samples visit cde.com/ulp
CDE
CORNELL
DUBILIER
ENERGIZING IDEAS

Editor Achim Scharf
Tel: +49 (0)892865 9794
Fax: +49 (0)892800 132
Email: PowerElectronicsEurope@t-online.de

Production Editor Chris Davis
Tel: +44 (0)1732 370340

Financial Manager Clare Jackson
Tel: +44 (0)1732 370340
Fax: +44 (0)1732 360034

Reader/Circulation Enquiries
Perception
Tel: +44 (0) 1825 701520
Email: dfamedia@dmags.co.uk

INTERNATIONAL SALES OFFICES

Mainland Europe:
Victoria Hufmann
Norbert Hufmann
Tel: +49 911 9397 643
Fax: +49 911 9397 6459
Email: pee@hufmann.info

Eastern US
Ian Atkinson
Tel: +44 (0)1732 370340
Fax: +44 (0)1732 360034
Email: ian@dfamedia.co.uk

Western US and Canada
Ian Atkinson
Tel: +44 (0)1732 370340
Fax: +44 (0)1732 360034
Email: ian@dfamedia.co.uk

Japan:
Yoshinori Ikeda,
Pacific Business Inc
Tel: 81-(0)3-3661-6138
Fax: 81-(0)3-3661-6139
Email: pbi2010@gol.com

Taiwan
Prisco Ind. Service Corp.
Tel: 886 2 2322 5266 Fax: 886 2 2322 2205

Publisher & UK Sales Ian Atkinson
Tel: +44 (0)1732 370340
Fax: +44 (0)1732 360034
Email: ian@dfamedia.co.uk
www.power-mag.com

Circulation and subscription: **Power Electronics Europe** is available for the following subscription charges. **Power Electronics Europe**: annual charge UK/NI £95, overseas $160, EUR 150.
Contact: DFA Media, 192 The High Street, Tonbridge, Kent TN9 1BE Great Britain.
Tel: +44 (0)1732 370340.
Fax: +44 (0)1732 360034. Refunds on cancelled subscriptions will only be provided at the Publisher's discretion, unless specifically guaranteed within the terms of subscription offer.

Editorial information should be sent to The Editor, **Power Electronics Europe**, PO Box 340131, 80098 Munich, Germany.

Printed by: Warners.

ISSN 1748-3530

FEATURE STORY

New Developments in RET Technology

Resistor-Equipped Transistors (RETs) – also known as digital transistors or pre-bias transistors – offer many benefits, including saving space, reducing manufacturing costs and increased reliability. Bipolar transistors are controlled using the base current. However, because the voltage drop across the base-emitter path is highly temperature-dependent, in most applications a series resistor is required to keep the base current at the desired level, thereby ensuring the stable and safe operation of the transistor. To reduce the component count and to simplify board designs, RETs combine single or dual bipolar transistors with the bias resistors which are integrated on the same die. Because these internal resistors have higher tolerances than commonly used external resistors, RETs are suitable for switching applications where the transistor operates in either on- or off-state. This is why RETs are often referred to as digital transistors. RETs are available in many voltage, current and resistance values, in NPN or PNP configuration and a variety of packages including SOT23 and SOT323 and SOT363. This article looks at their structure and design considerations, and considers the suitability of new, 80 V parts that target emerging 48 V EV systems.

Cover image supplied by Nexperia

The Year of Power GaN

Global investment in renewable energy capacity moved up 2 % to $303 billion in 2020. This was the second-highest annual figure ever (after 2017's $313.3 billion), and the seventh consecutive total of more than $250 billion. A geographical split of BNEF's energy transition investment data shows that Europe accounted for the biggest slice of global investment, at $166 billion (up 67 %), with China at $135 billion (down 12 %) and the USA at $85 billion (down 11 %). Europe's impressive performance was driven by a record year for electric vehicle sales, and the best year in renewable energy investment since 2012.

Silicon devices such as IGBTs are benefiting from mature infrastructure and processes. New device generations are coming to the market. In addition to performance improvements, Si IGBT costs will further be reduced thanks to a 12-inch Si wafer transition that will make the competition with WBG materials even tougher. In 2019 the whole power semiconductor device market segment was worth $17.5 billion, with an expected CAGR by market researcher Yole for 2019-2025 of 4.3 %. IGBT modules, which represented $3.7 billion in 2019, are traditionally used in applications such as industrial or renewable energy converters. These applications are today driven by efficiency regulations or increasing clean energy goals, and they account for 46 % of the total IGBT module market. Nevertheless, the key application for power IGBT modules is undoubtedly EV/HEV, with an expected growth of 18 % from 2019 to 2025.

Following Tesla's adoption of SiC in its Model 3 main inverter, automotive has become the killer application for SiC, according to Yole. Since then, SiC has entered the priority list of almost all carmakers. While Chinese BYD has also chosen SiC in its premium models in 2020, Audi, Volkswagen, and Hyundai are expected to adopt SiC in their next generation models. Despite the global slowdown in H1-2020 due to the Covid-19 outbreak, design wins for SiC solutions have recently multiplied, with a bright market outlook for 2019-2025 period. In this context, the SiC automotive market is expected to grow to exceed $1.5 billion in 2025, with a 38 % CAGR. Along with EV applications, SiC is of great interest to the charging infrastructure market, which is growing significantly. High-power traction inverters represent a huge new business opportunity for suppliers of SiC devices, suitable device packaging solutions, and SiC-based systems. Also, interest in GaN has recently revived, mainly as a potential candidate for future EV/HEV 12 – 48 VDC converters and onboard chargers.

2021 will see more 48 V battery systems, particularly in mild hybrids, as manufacturers add active suspension, rear wheel steering or antiroll stabilization systems, expects Vicor. Supporting this move, more 48 V systems will need to convert down to 12 V to support car safety, comfort, infotainment, and navigation systems. In addition to enabling lighter cabling or delivering higher power, the conversion from the high-voltage batteries in HEVs and EVs is more efficient when the step down required is reduced by increasing the voltage to 48 V. Primary battery voltages used to power EVs and HEVs will also increase in voltage with 800 V becoming much more common allowing faster charging time. These changes demand a new class of power components to create the power distribution network within next year's automobiles. Regarding automotive in 2021 GaN Systems foresees advances in power systems with GaN technology and battery technology which are driving significant OEM and Tier 1 supplier adoption for EVs and addressing past concerns around range anxiety and car purchase price. The story of GaN in EV's will shift to become more of a narrative about enhanced performance and new capabilities for vehicle designs. By 2025, one of every 10 vehicles sold worldwide will be a 48 V mild hybrid, expects EPC. 48 V systems boost fuel efficiency by 10-15 % delivering 4X the power without increasing engine size, and carbon-dioxide emissions by 25 %.The need for 48 V bus power distribution becomes increasingly evident with all the new power hungry electronically driven functions and features appearing on the latest cars such as electric start-stop, electric steering, electric suspension, electric turbo-supercharging, or variable speed air conditioning. And now, with the emergence of autonomous vehicles, additional demands from lidar, radar, camera, and ultrasonic sensors, are placed upon the power distribution system. These require high performance graphic processors to gather, interpret, integrate, and to make sense of it all. These processors are very power hungry and put an additional burden on traditional automotive 12 V electrical distribution buses. For 48 V bus systems, GaN technology increases the efficiency, shrinks the size, and reduces system cost. Due to the fast switching speed GaN-based solutions can operate at 250 kHz per phase as oppose to 125 kHz for traditional MOSFET solutions, reducing both size and cost.

Thus, after ten years of its market introduction, 2021 is seen as the year of GaN, not only in automotive. We at Power Electronics Europe have inspired the power electronics community to implement new technologies and devices over the years and will continue to do so.

Enjoy reading this issue!

Achim Scharf
PEE Editor

Graphene Heat Pipe Increases Thermal Conductivity

Heat pipes are usually made of copper or aluminum. However, due to their relatively high density and limited heat transmission capacity, such heat pipes are facing challenges in power electronics. The newly researched graphene enhanced heat pipe featuring graphene assembled film with nanostructure enhanced inner surfaces improve heat dissipation capacity about 3.5 times higher. Involved were researchers in Sweden, China and Italy.

"Heat pipes are one of the most efficient tools for this because of their high efficiency and unique ability to transfer heat over a large distance," says Johan Liu, Professor of Electronics Production, at the Department of Microtechnology and Nanoscience at Swedish Chalmers University. And, compared to metal materials, graphene shows overwhelming advantages such as lightweight, good stability and superior in-plane thermal conductivity (up to 5000 W m-1 K-1 at room temperature), far better than that of copper (402 W m^{-1} K^{-1}) and aluminum (237 W m^{-1} K^{-1}). Furthermore, compared with single layer graphene film, graphene assembled films (GF) reach a good compromise between thermal conductivity, scalable preparation and applicable mechanical strength. GF with thickness at 1–2 microns has exhibited thermal conductivities up to 2500 W m^{-1} K^{-1} and tensile strength of 78 ± 6 MPa. More importantly, GF has little corrosion risks even under acid, alkali and moisture exposure than metal based materials. Taken all of these advantages into consideration, graphene possesses promising potential to boost heat dissipation performance of heat pipes.

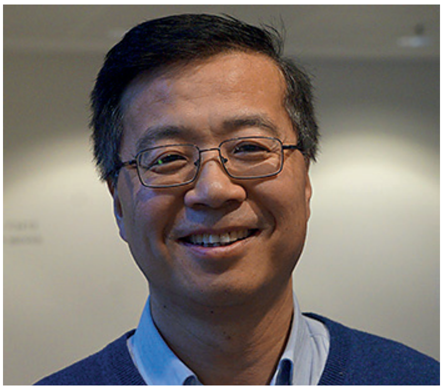

"The graphene-enhanced heat pipe exhibits a specific thermal transfer coefficient which is about 3.5 times better than that of copper-based heat pipe", states Chalmers-University Prof. Johan Liu

Design of graphene heat pipe

A recently demonstrated graphene heat pipe (GHP) at Chalmers University of Technology in Sweden exhibits a cooling capacity up to 7230 W m^{-2} K^{-1} g^{-1} under a 10 W heat loading, which is about 3.5 times better than that of commercial copper based heat pipes with the same geometry (2053 W m^{-2} K^{-1} g^{-1}). Besides, simulation results reveal that the GF contributes over 30 % to the total heat dissipation ability of the heat pipe due to its outstanding thermal conductivity. Heat transfer modeling suggests that increasing thermal conductivity of wall material (container) can significantly improve its heat dissipation capacity.

The GHP consists of three key components, including container, wick structure and working fluid (Figure 1A, B). To improve the mechanical strength of the GHP container, a copper spring was inserted. On one hand, the ultra-high in-plane thermal conductivity of graphene film endows heat conduct from the evaporator section to the condenser section rapidly. On the other hand, the working fluid is evaporated when heat enters GHP at its evaporator section. The evaporated fluid creates a pressure gradient to force the vapor to move towards the condenser section. While vapor reaches the condenser section, the vapor condenses and releases its latent heat of evaporation by external devices that is, heat sink. After that, the working fluid is relatively or passively pumped to the evaporator section for re-evaporation by the capillary force of wick structure (Figure 1C). Thus, by using this liquid-vapor phases changes, heat transport in GHP becomes extremely fluent and efficient.

Design and image of the GHP (A, image of a real GHP; B, schematic designing of the GHP; C, working principle of the GHP)

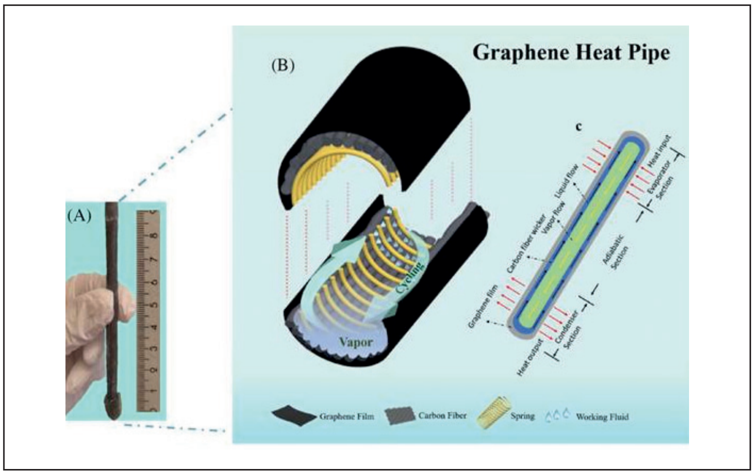

Heat dissipation performance

GHPs with various lengths (90, 130, 150 mm) were fabricated to investigate the relationship between length and specific thermal transfer coefficient. When the length of the 6 mm outer-diameter GHP decreases from 150 to 90 mm, temperature on the evaporator section decreases from 77°C to 42°C (Figure 2 A-C) with 10 W heat loading. Meanwhile, the g increases with shortened length of GHP and reaches 7230 W m-2 K-1 g-1 with a heat loading of 10 W (Figure 2D). It is demonstrated that the heater temperature decreases with shortened pipe length (Figure 2E), consistent with the trends of g. With a 10 W heat loading, temperature of the heater containing a 90 mm GHP goes to 42°C with a 15.4 mins start-up time in steady state (Figure 2F, T4 is the temperature at thermal couple 4), far lower than that (86°C) of the independent heater without graphene pipe. These provide evidence that shorter GHP carries more power than longer pipe since capillary limit is an inverse function of the length. On the other hand, the start?up time of GHP significantly shorts with higher heat loading. Such tendency is because higher heat loading provides sufficient pressure difference between inlet and outlet of evaporator section to activate the GHP.

The contributions from the container's thermal conductivity and phase change process were assessed numerically by COMSOL Multiphysics solver. Models of 6 mm outer diameter GHPs with length of 90, 130, and 150 mm have been designed. In particular, thermal conductivity of container was set as 400, 900, and 1400 W m^{-1} K^{-1} to figure out the contribution from the container in a GHP. Similar to the experimental results, it was found that the shorter GHP, the lower temperature is on the heat pipe. Additionally, with the same GHP diameter and length, the temperature on the heater decreases by improving the thermal conductivity of GF. This observation implies that improving thermal conductivity of the container would effectively promote heat dissipation of GHP.

A commercial copper heat pipe with the same diameter (CHP, Spread Fast AB, 6 mm) was used as a reference to evaluate the thermal dispassion behavior of GHP. In the CHP, copper and sintered copper powder works as container and wick structure (Figure 2G). Similar temperature distribution and start-up behavior are observed from GHP and CHP, as shown in Figure 3H. While compared to CHP, the start-up time of GHP decreases 35 %. Such improvement maybe because the rough and flexible surface property of GF, which decrease contact resistance between the heat pipe and heat source. Moreover, the GHP shows a significant advantage on specify thermal transfer coefficient (Figure 2I). A standard 90 mm GHP weights 2.1 g while the weight of the same diameter CHP is 12.9 g. The specific thermal transfer coefficient of GHP is improved by 3.5 times compared to that of the CHP. Therefore, such a high specific thermal transfer coefficient makes GHP an ideal candidate for thermal management on lightweight applications such as in spacecraft, avionics, automotive and consumer systems where performance versus weight is of great concern.

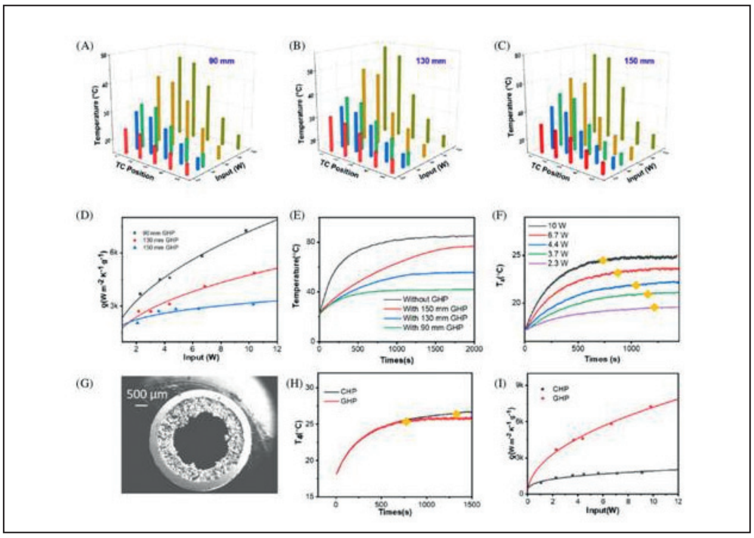

Heat dissipation performance of a 6 mm GHP (A, B, C, temperature distribution along GHP with lengths of 90, 130, and 150 mm; D, specific thermal transfer coefficient of GHP with length of 90, 130, and 150 mm (R^2 = 0.98607, 0.96344, 0.84614); E, temperature distribution on heater with 90, 130, and 150 mm GHP under 10 W input; F, start-up times of 90 mm GHP under various heat loading; G, cross?section SEM image of CHP; H, start-up times of GHP and CHP with 10 W heat loading; I, specific thermal transfer coefficient of GHP and CHP) ¶

Literature

A lightweight and high thermal performance graphene heat pipe
https://doi.org/10.1002/nano.202000195

Hot Salt Rechargeable Battery

Using salt as a key ingredient, Chinese and British researchers have designed a new type of rechargeable battery that could accelerate the shift to greener electric transport.

Many electric vehicles (EV) are powered by rechargeable lithium-ion batteries, but they can lose energy and power over time. Under certain conditions, such batteries can also overheat while working or charging, which can also degrade battery life and reduce miles per charge. To solve these issues, the University of Nottingham is collaborating with six scientific research institutes across China to develop an innovative and affordable energy store with the combined performance merits of a solid-oxide fuel cell and a metal-air battery. The new battery could significantly extend the range of electric vehicles, while being fully recyclable, environmentally-friendly, low-cost and safe.

A solid-oxide fuel cell converts hydrogen and oxygen into electricity as a result of a chemical reaction. While they are highly-efficient at extracting energy from a fuel, durable, low-cost and greener to produce, they are not rechargeable. Meanwhile, metal-air batteries are electrochemical cells that uses a cheap metal such as iron and the oxygen present in air to generate electricity. During charging, they emit only oxygen into the atmosphere. Although not very durable, these high-energy dense batteries are rechargeable and can store and discharge as much electricity as lithium-ion batteries, but much more safely and cheaply.

In the early research phases, the research team explored a high-temperature, iron-air battery design that used molten salt as a type of electrolyte - activated by heat - for electrical conductivity. Cheap and inflammable, molten salts help to give a battery impressive energy storage and power capability and a lengthy lifecycle.

Key nano-technology

However, molten salts also possess adverse characteristics. University of Nottingham study lead, Prof. George Chen said: "In extreme heat, molten salt can be aggressively corrosive, volatile and evaporate or leak, which is challenging to the safety and stability of battery design. There was an urgent need to fine-tune these electrolyte characteristics for better battery performance and to enable its future use in electric transport." The researchers have now improved the technology by turning the molten salt into soft-solid salt, using solid oxide nano-powders.

The novel quasi-solid-state (QSS) electrolyte, consisting of the molten eutectic mixture of Na2CO3-K2CO3 and nanoparticles of yttrium stabilized zirconia (YSZ) in a mass ratio of 1:1. The QSS electrolyte has relatively lower volatility in comparison with the pristine molten Na2CO3-K2CO3 eutectic, and therefore significantly suppresses the evaporation of molten salts, thanks to a strong interaction at the interface between molten salt and YSZ nanoparticles at high temperatures. The QSS electrolyte was used to construct an iron-air battery that performed excellently in charge-discharge cycling with high columbic and energy efficiencies. Also a redox mechanism at the three-phase interlines in the negative electrode appears. These findings can help establish a simpler and more efficient approach to designing low-cost and high-performance molten salt metal-air batteries with high stability and safety.

Prof. Jianqiang Wang, from the Shanghai

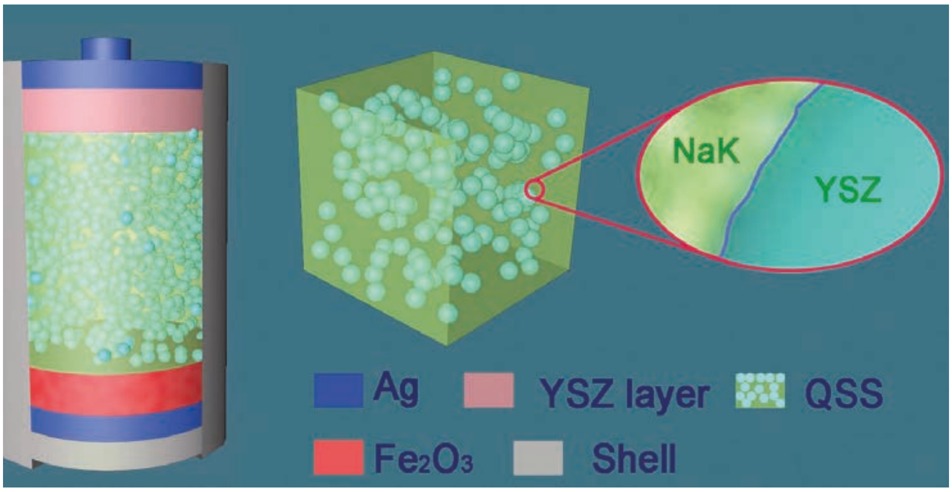

The novel QSS electrolyte in the salt battery consists of the molten eutectic mixture of Na_2CO_3-K_2CO_3 and nanoparticles of yttrium stabilized zirconia (YSZ)

Institute of Applied Physics, Chinese Academy of Sciences, who is leading this collaboration project has predicted that this QSS electrolyte is suitable for metal-air batteries which operate at 800°C; as it suppresses the evaporation and fluidity of the molten salts that can occur at such high operating temperatures. Project collaborator, Dr Cheng Peng from the Shanghai Institute of Applied Physics, explains a unique and useful design aspect of this experimental research. "The quasi-solidification has been achieved using nano-technology to construct a flexibly-connected network of solid oxide particles that act as a structural barrier locking in the molten salt electrolytes, while still allowing them to safely conduct electricity in extreme heat."

Prof. Chen hopes the team's "encouraging results" will help to establish a simpler and more efficient approach to designing low-cost and high-performance molten salt metal-air batteries with high stability and safety. "The modified molten salt iron-oxygen battery has great potential applications in new markets, including electric transport and renewable energy which require innovative storage solutions in our homes and at grid-level. The battery is also, in principle, capable of storing solar heat as well as electricity, which is highly-desirable for both domestic and industrial energy needs. Molten salts are currently used at large scale in Spain and China to capture and store solar heat which is then converted to electricity - our molten salt metal air battery does the two jobs in one device," he added.

More information: George.chen@nottingham.ac.uk

World Invested Unprecedented Amounts in Low-Carbon Assets

According to a new measure of 'energy transition investment', compiled by BloombergNEF (BNEF), shows that the world committed a record $501 billion to decarbonization in 2020, beating the previous year by 9 percent despite the economic disruption caused by the Covid-19 pandemic.

BNEF's analysis shows that companies, governments and households invested $303 billion in new renewable energy capacity in 2020, up 2 % on the year, helped by the biggest-ever build-out of solar projects and a $50 billion surge for offshore wind. They also spent $140 billion on electric vehicles and associated charging infrastructure, up 28 % and a new record. Other areas of energy transition investment also showed strength. Domestic installation of energy-efficient heat pumps came to $51 billion, up 12 %, while investment in stationary energy storage technologies such as batteries was $3.6 billion, level with 2019 despite falling unit prices. Global investment in carbon capture and storage (CCS) tripled to $3 billion, and that in hydrogen was $1.5 billion. "Our figures show that the world has reached half a trillion dollars a year in its investment to decarbonize the energy system. Clean power generation and electric transport are seeing heavy inflows, but need to see further increases in spending as costs fall. Technologies such as electric heat, CCS and hydrogen are only attracting a fraction of the investment they will need in the 2020s to help bring emissions under control. We need to be talking about trillions per year if we are to meet climate goals", commented Albert Cheung, head of analysis at BNEF. Global investment in renewable energy capacity moved up 2 % to $303 billion in 2020. This was the second-highest annual figure ever (after 2017's $313.3 billion), and the seventh consecutive total of more than $250 billion.

A geographical split of BNEF's energy transition investment data shows that Europe accounted for the biggest slice of global investment, at $166 billion (up 67 %), with China at $135 billion (down 12 %) and the USA at $85 billion (down 11 %). Europe's impressive performance was driven by a record year for electric vehicle sales, and the best year in renewable energy investment since 2012.

https://about.bnef.com/

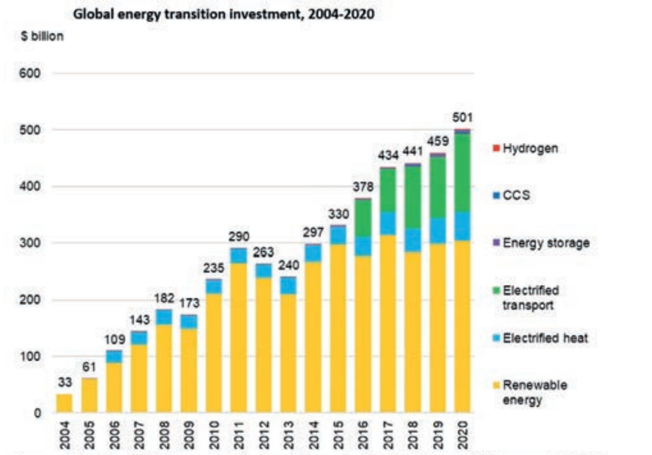

Source: BloombergNEF. Note: electrified heat figures begin in 2006; electrified transport in 2016; hydrogen and CCS in 2018.

Hybrid Electric Vehicles: A Stay of Execution for NiMH Batteries

In battery-electric vehicles, the lithium-ion battery is dominant; however, for full hybrid electric vehicles (those that have electric-only modes but do not plug-in), NiMH batteries are still the most common battery on the road. With the growing market for hybrid electric vehicles (HEVs), will this drive further demand for NiMH batteries and stop them from being eliminated from the automotive market?

Toyota is the ruling OEM in the global HEV car market, with over 60 % market share in 2019. Other manufacturers have started to eat into this share over the years, but Toyota still reigns supreme. While the other OEMs have mostly transitioned towards Li-ion batteries for their HEVs, Toyota remains committed to NiMH batteries and HEVs for the foreseeable future, with the majority of their line-up now using either NiMH or Li-ion depending on the specifications. For the relatively small batteries that are used in HEVs, the NiMH is still sufficient to meet requirements. It is also much more technologically mature and lower cost than Li-ion. Sales of HEVs have continued to grow throughout the COVID-19 pandemic despite the downturn of the overall car market. This, combined with Toyota's dominance and NiMH portfolio, provides a good market for NiMH batteries, at least in the short term. Li-ion technology is still evolving and reducing in price; at a certain point, it may no longer be cost-effective to continue using NiMH. Additionally, fossil fuel bans are incoming, with countries like the UK banning purely internal combustion engine (ICE) vehicles by 2030 and only allowing hybrids "that can drive a significant distance with zero emissions". HEV manufacturers will likely increase the battery capacity in order to give more electric-only range, making the Li-ion option more appealing. Even with this stay of execution for HEVs, banning vehicles with ICEs of any sort is likely to follow shortly after. This will eliminate the HEV in many markets and hence the demand for NiMH.

IDTechEx recently published the report "Full Hybrid Electric Vehicle Markets 2021-2041". This report gives an in-depth look at the historic HEV market in China, Europe, Japan, South Korea, and the US, with an outlook over the next 20 years.

The electric truck market in the US is primed for huge growth. Having largely lagged behind China and Europe in electric commercial vehicle deployment, the transition to zero-emission vehicles in this sector now seems set to begin in earnest. The IDTechEx report, "Electric Truck Markets 2021-2041" contains twenty-year regional forecasts for the battery electric and fuel cell truck markets. US President Biden's announcement, alongside factors such as the California Air Resources Board's Advanced Clean Trucks regulation, which last year mandated that 75 % of new Class 4-8 ridged truck and 55 % of new tractor truck sales in California must be zero-emission by 2035 and growing evidence of significant demand for commercial EVs from major US corporations, should give great confidence to truck manufacturers and their supply chain that the market for electric trucks will be worth the resources and investment that is necessary to transition away from the combustion engine.

A great deal of attention is given to whether battery electric trucks will be able to offer the range to make long-haul trucking applications viable with an electric powertrain. This question will be addressed to some extent by the first delivery of Tesla Semi trucks, which at least provisionally is still penciled in for 2021 (though production timelines have slipped on multiple occasions). While the mass of batteries required and the likely need for ultra-fast charging undoubtedly make long haul EV trucking a challenge, there is a significant market for medium and heavy-duty trucks that do not require extensive range. Swedish heavy-duty truck and bus manufacturer Scania's recent forecasts highlight how quickly the market is progressing around the world. By 2025 they expect 10 % of their total vehicle sales will be electric vehicles, rising to 50 % of sales by 2030.

The lithium-ion batteries in electric vehicles (EVs) present very different material demands at the cell- and pack-level compared with the internal-combustion engine (ICE) vehicles they replace. Whilst ICE drivetrains heavily rely on aluminum and steel alloys, Li-ion batteries utilize a lot of materials such as nickel, cobalt, lithium, copper, insulation, thermal interface materials, and much more at a cell- and pack-level. The markets for these materials will see a rapid increase in demand that would not have been present without the take-off of electric vehicle markets. OEMs are changing the way they make batteries. Improvements to energy density are one key consideration but also the sustainability of the materials used. Many materials involved have questionable mining practices or volatile supply chains. One such material is cobalt, which in addition to being very expensive, has its supply and mining confined mostly to China and the Democratic Republic of Congo. As a result, OEMs are trending towards higher nickel cathode chemistries like NMC 622 or NMC 811 in some new models.

Up until 2018, the Chinese electric car market was predominately using LFP cathodes. This has now transitioned such that, as of 2019, only 3 % of cars utilized LFP batteries. However, Tesla has now introduced the LFP Model 3 made in China, which could upset this trend. Additionally, LFP is used extensively for markets like Chinese electric buses. Despite the reduction in market share of materials like cobalt, the rapidly increasing market for electric vehicles will drive demand for cobalt and many other materials drastically higher over the next 10 years. A new report from IDTechEx, "Materials for Electric Vehicle Battery Cells and Packs 2021-2031", identifies and analyzes trends in the materials used for the assembly and production of battery cells and battery packs in the EV market.

www.IDTechEx.com

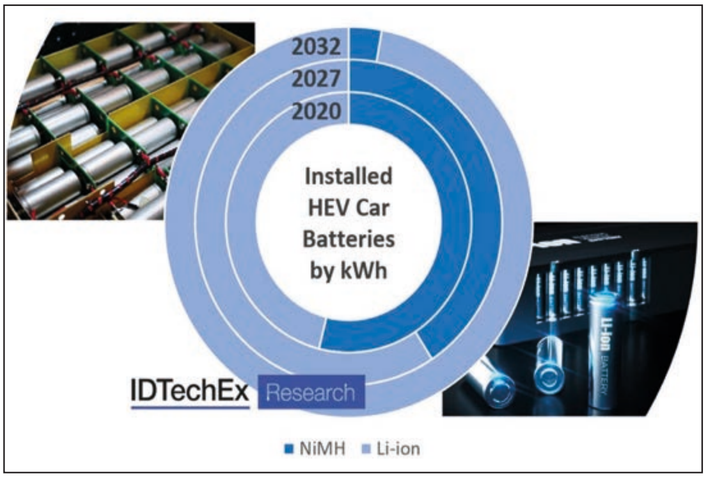

Power Electronics Drive (H)EV Markets

Driven by the prosperous EV/HEV market, the market for power semiconductor electronics should have a bright future, with value exceeding $3.7B in 2024 at a 2018 - 2024 Compound Annual Growth Rate (CAGR) of 21 percent. In competition with Silicon, SiC and GaN have made remarkable progress in the power electronics business over the last decade.

IGBT modules represent the largest market, which is expected to double in five years. Silicon carbide (SiC) power modules will also grow fast, with a 2018 - 2024 CAGR of 48 %, according to market researcher Yole. The power module is one of the key elements in power converters and inverters. The market for power modules will reach $7.6 billion by 2025, with a 2019-2025 CAGR of 9.1 %. In the past, packaging needs were driven by industrial applications, but today they are increasingly driven by EV/HEVs. In fact, by 2025 EV/HEVs will become the biggest power module market, representing a market value of almost $3.4 billion. This market's promising outlook is beneficial for the power module packaging material business. The power module packaging material market will achieve a 2019-2025 CAGR of 11 %, being worth $2.7 billion by 2025. Following Tesla's adoption of SiC in its main inverter, automotive has become the killer application for SiC. Since then, SiC has entered the priority list of almost all carmakers. While Chinese BYD has also chosen SiC in its premium models in 2020, Audi, Volkswagen, and Hyundai are expected to adopt SiC in their next generation models. Despite the global slowdown in H1-2020 due to the Covid-19 outbreak, design wins for SiC solutions have recently multiplied, with a bright market outlook for 2019-2025 period.

In this context, the SiC automotive market is expected to grow to exceed $1.5 billion in 2025, with a 38 % CAGR. Along with EV applications, SiC is of great interest to the charging infrastructure market, which is growing significantly. Indeed, high power chargers can benefit from SiC's higher efficiency and higher frequency by offering more compact solutions than Silicon IGBTs. The market size is expected to reach $225 million in 2025 with a 90 % CAGR between 2019 and 2025.

Besides automotive, applications such as PV, rail and motor drives will also show double-digit CAGR in the 2019-2025 period.

High-power traction inverters represent a huge new business opportunity for suppliers of SiC devices, suitable device packaging solutions, and SiC-based systems. Also, interest in GaN has recently revived, mainly as a potential candidate for future EV/HEV 12 – 48 VDC converters and onboard chargers. "Tier 1s are increasing their efforts in EV/HEV-related products. However, OEMs are becoming more and more intrusive, particularly in main inverters, with the objective of controlling the key EV/HEV elements. Established semiconductor device suppliers are in a similar situation, on the one hand facing the entrance of some Tiers 1s in the device market, and addressing challengers from the emergence of WBG devices on the other", commented analyst Milan Rosina.

More generally, the market outlook for SiC devices looks promising. This market will reach a 30 % CAGR for the 2019-2025 period, according to Yole' Power SiC report 2020. Since the commercialization of the first SiC device in 2001, SiC devices performances and the value have been gradually proven. Their price has also become increasingly attractive for the end users.

For the GaN power market, the adoption of GaN HEMTs for Oppo's in-box fast charger at the end of 2019 boosted the penetration of this material. Indeed, several phone makers such as Vivo, Realme and Meizu rushed to adopt GaN-based in-box fast chargers for their flagships released in early 2020. Also other players, such as Samsung and Xiaomi, have opted for GaN accessory chargers. "The GaN journey has just started with the end-consumer mass market where it will gain volume production. In a few years, it will also expand in the automotive and industrial market", said analyst Ahmed Ben Slimane.

www.yole.fr

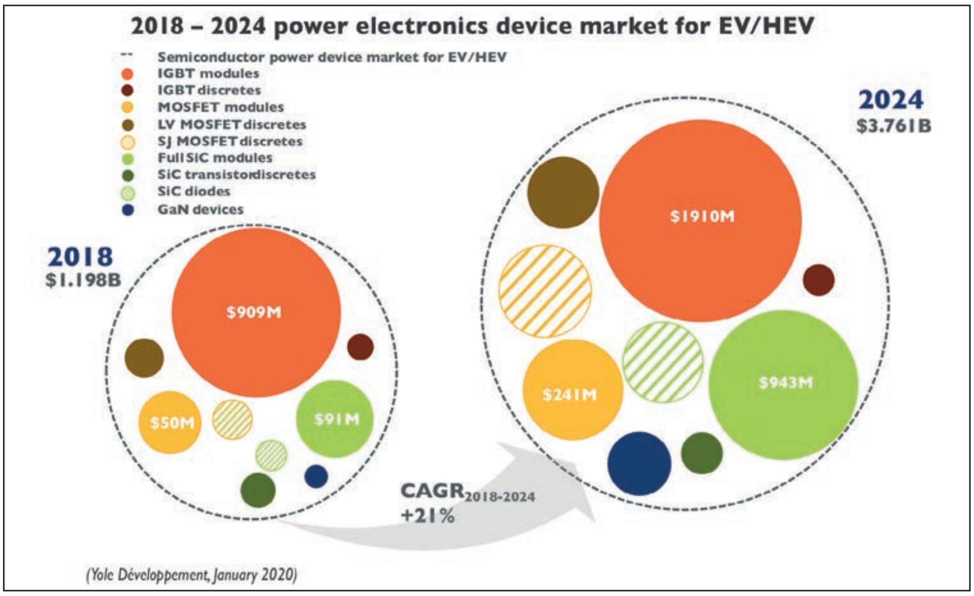

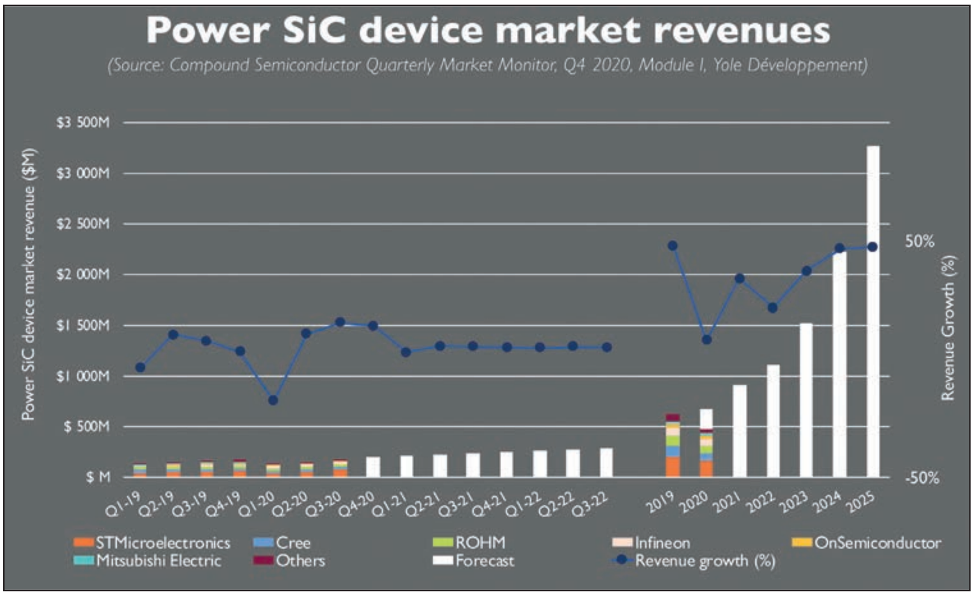

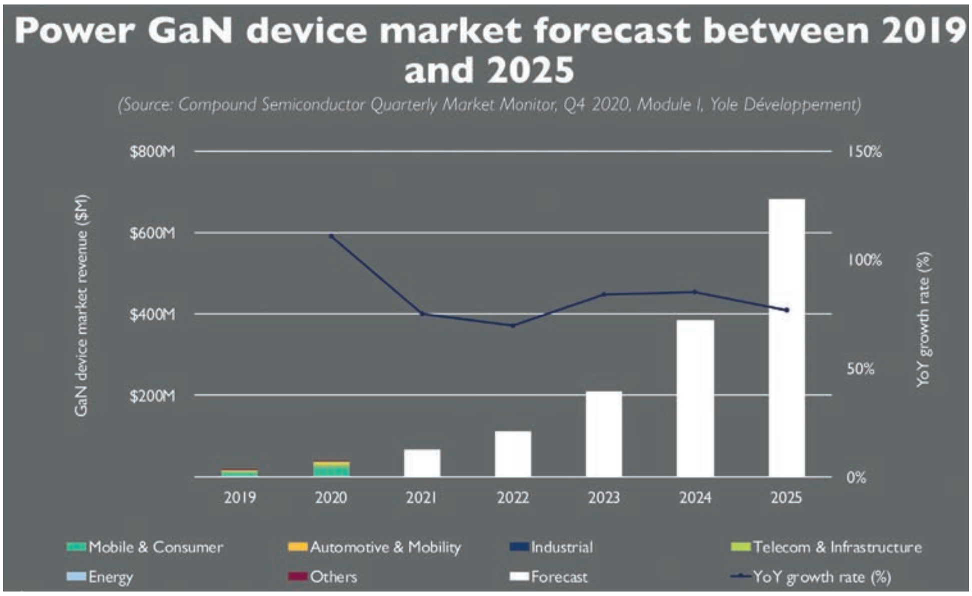

GaN System's 2021 Technology Predictions

GaN Systems is more convinced than ever that Silicon has reached its limitations in solving critical power systems challenges. GaN transistors are the clear solution for driving more robust growth and product innovation in the electronics industry.

"Major companies are designing and shipping products with GaN today. In 2021, we will see significantly increased demand for and adoption of GaN-powered products across multiple markets - especially in consumer products and industrial power supplies. The high reliability of GaN power transistors and their ability to bring economic advantage to many applications will be ever more common over the next twelve months – and beyond", said marketing manager Paul Wiener. "In 2020, the conversation around GaN technology began to shift from a focus on early adopters and risk - to one of proven reliability and market acceptance. This is the result of products with GaN semiconductors finding success in consumer markets with power adapters and audio, renewed and reenergized work with GaN technology in EV design labs, new EU policy standards around energy efficiency in data centers that only GaN technology can effectively address when combined with power density expectations, and important industry accomplishments in product reliability. 2021 will be the year that GaN technology further demonstrates that it has successfully shifted from early adoption by claiming a substantial and publicly visible foothold in power-reliant markets as diverse as automotive, data centers, and consumer electronics."

Regarding automotive in 2021 GaN Systems foresees advances in power systems with GaN technology and battery technology which are driving significant OEM and Tier 1 supplier adoption for EVs and addressing past concerns around range anxiety and car purchase price. The story of GaN in EV's will shift to become more of a narrative about enhanced performance and new capabilities for vehicle designs. Traditionally, automotive manufacturers have been conservative in their adoption of new technology. In 2021, governments and the public will continue to demand EV's with price and range similar to today's ICE vehicles. Manufacturers will benefit from embracing GaN's proven and noteworthy reliability and cost-efficiency in delivering their designs for these vehicles.

Regarding CHARGERS and ADAPTERS 2020 was the year of the GaN charger. The aftermarket saw more than 100 new models of chargers and adapters in the market for phones, tablets and handheld gaming devices. Looking ahead to 2021, this will be the year of GaN chargers from OEM's, along with the rise of multiport adapters. GaN chargers are moving from a once niche position to the mainstream standard, while also being positioned to deliver on future evolving customer needs with advances in device design, performance, energy efficiency, and power requirements.

Regarding Data Centers in 2021 GaN Systems foresees that the global economy remains on its way to its "digital destiny" as most products and services are now based on a digital delivery model or require digital augmentation to remain competitive. The data center ecosystem will continue to evolve and become even more critical for organizations. Infrastructure efficiency has been a huge concern for many organizations. While 2020 was the year of significant increase in GaN power supply design efforts, we predict that 2021 will focus on actual implementation of GaN in data centers. Smaller power supplies using GaN technology allow for more storage and memory to be added into the same rack space allowing for data center capacity growth without actually having to build more data centers.

www.gansystems.com

Vicor's 2021 Technology Predictions

Buried in the tumult of 2020 was a rapid acceleration in the speed of innovation. Nowhere was this more evident than in the record-breaking development of not one, but many, COVID-19 vaccines. The accelerating speed of innovation is also happening in other fields, driven by changing habits and reset priorities due to the pandemic.

"Covid has accelerated move to Electric Vehicles and Migration to 48V systems", said Nicolas Richard, Vicor's Director of EMEA Automotive Business Development. "2021 will see more 48 V battery systems, particularly in mild hybrids, as manufacturers add active suspension, rear wheel steering or antiroll stabilization systems. Supporting this move, more 48 V systems will need to convert down to 12 V to support car safety, comfort, infotainment, and navigation systems. In addition to enabling lighter cabling or delivering higher power, the conversion from the high-voltage batteries in HEVs and EVs is more efficient when the step down required is reduced by increasing the voltage to 48 V. Primary battery voltages used to power EVs and HEVs will also increase in voltage with 800 V becoming much more common allowing faster charging time. These changes demand a new class of power components to create the power distribution network within next year's automobiles".

"Data Center Capacity Demand Will Exceed Physical Plant Space", expects Lev Slutskiy, Vicor's Regional Manager. "In 2021, the quest for more power efficiency in the datacentre will step up a gear where we believe not only will the datacenter industry purchase more renewable energy than in previous years, but we anticipate more datacenters moving away from AC in favor of DC infrastructure solutions to better cope with the massive increases in power demands of high-performance computing. A more efficient way to manage power is to increase the voltage within these systems and to use renewable energy. The task of conversion of the high voltage (usually 260 – 410 V DC) to the values used at the input of modern computing units (12V or better 48V) could be performed by bus converters. We believe that system designers will use more of these innovative architectural solutions, such as Factorized Power Architectures (FPAs), and efficient converter modules to shorten

the distances between the high current supplier module to the point of load (PoL), to lower PDN resistance which will minimize power loss in future supercomputing applications. Several major high-performance computing (HPC) manufacturers have moved over to this approach in effect turning the datacenter green from the inside out."

"By the end of 2021, for every European there will be at least one sighting of a delivery robot or drone on its way to dropping off a package or disinfecting public spaces as a part of our fight against the pandemic", anticipates Henryk Dabrowski, VP Sales for Vicor in EMEA. "One of the key factors to expanding automated delivery services will be range and weight of the robot or drone. Vicor enables designers to lighten their drones for performance and manage power in such a way that the drones can fly further and more reliably than ever before. We predict that denser populations in Europe's cities will see many more bots than drones, while more remote areas such as Alps will see more drones help with crisis issues and delivery of vital medical supplies, while heavier deliveries will be supported by autonomous trucks. In Europe, Tescos, Amazon, DHL and UPS have all began trials with delivery drones and we see the recent pandemic as the tipping point to push retail towards a complete digital transformation. The convenience of home delivery that people have become accustomed to during lockdown will mean that in-person shopping at your favourite store or supermarket will not return to pre-pandemic levels. The use of robots rolling around the streets, and drones in the air will enable retailers to provide deliveries at even lower cost. In China, drones have already begun deliveries to remote parts of the country, and we see accelerated progress with logistics companies achieving permissions from national flight authorities to allow for retail air travel via drone."

www.vicorpower.com

Powerex Announced New CEO/COO

Joseph Wolf (left in picture) has been appointed as President and Chief Executive Officer. He will succeed the outgoing CEO, John Hall, who has retired. Joe has been serving as a Vice President and the company's Chief Financial Officer since 2016.

Joe joined Powerex as a Sr. Financial Analyst in 2008. He steadily progressed in leadership roles during his tenure at the company rising from Controller to Director of Finance to CFO and now CEO. He is the right executive to lead the company during the challenging post-COVID-19 recovery and is pro-actively pursuing numerous opportunities to solidify Powerex as a premier supplier and trusted industry partner. He is equally committed to personal and professional growth of the highly dedicated Powerex Team members.

In a related move, Ronald Yurko (right in picture) has been promoted from company Vice-President to Chief Operating Officer (COO). Ron joined Powerex in 2007 as an Engineering Manager. Ron was promoted to running the R&T Business Unit in 2010. In subsequent years he has taken on more responsibility in Sales and in helping forge company strategy. His strong Engineering and Manufacturing background, his Sales abilities, and his reputation with Powerex customers makes him an ideal choice for COO.

Powerex is a joint venture between General Electric and Mitsubishi Electric with corporate headquarters and manufacturing located in Youngwood, Pennsylvania. The company was founded in 1986 and can trace its origins back to Westinghouse Electric, which established the facility at the current location in 1956. The 90,000 square feet of manufacturing space includes Silicon wafer processing, diffusion, assembly, test, and high reliability screening. Powerex also features a semi- automated manufacturing power module line in a Class 10,000 cleanroom. Its broad product line includes SiC MOSFETs, IGBTs, HVIGBTs, rectifiers, thyristors, custom power modules and assemblies. These highly reliable electronic component solutions are designed for the Defense, Aviation, Traction, Mining, Medical, and Renewable Energy markets.

www.pwrx.com

Nexperia Increases Global Power Semiconductor Production and R&D

Nexperia will be making significant additional global investments in manufacturing capacity and research and development during 2021. The new investments are in line with a growth strategy that last year saw Wingtech Technology, Nexperia's parent company, commit $1.85 billion to building a new 300 mm (12-inch) power semiconductor wafer fab in Lingang, Shanghai. This factory, which will go live in 2022, will have an estimated annual output of 400,000 wafers.

Nexperia's plans for this year include improving production efficiency and implementing new 200 mm technologies at its European wafer fabs in Hamburg/Germany and Manchester/UK. In Hamburg there will also be additional investment in new technology for wide bandgap semiconductor manufacturing. New product development will be supported with a commitment to an increased R&D investment to approximately 9 % of total sales. Nexperia recently opened new global R&D centers in Penang in Malaysia and Shanghai in China and expanded the existing R&D sites in Hong Kong, Hamburg and Manchester. The company will also enhance test and assembly capabilities at factories in Guangdong in China, Seremban in Malaysia and Cabuyao in the Philippines, including the implementation of advanced automation and system-in-package (SIP) capabilities. "Increased vehicle electrification, 5G communications, Industry 4.0 and the mainstream adoption of GaN-based designs will all drive increased demand for power semiconductors in 2021 and beyond. Since we ship more than 90 billion units annually, the additional global investment will ensure that we continue to provide the technology and manufacturing capacity needed to deliver products in volumes that support future demand," said CEO Achim Kempe. "Since Wingtech's acquisition of Nexperia in 2019 we have committed to ongoing investment to support ambitious growth plans and capitalize on the synergies between the two businesses. Followig and Shanghai we are continuing with investments that support our growth across the globe," added Xuezheng Zhang (Wing), CEO of Wingtech and Nexperia.

www.nexperia.com/about

Optimistic for FY 2021

2021 fiscal year off to a good start for Infineon. Target markets showing dynamic momentum, outlook for the year raised slightly. Production start in Villach for power semiconductors brought forward.

Revenue for the three-month period increased from €2,490 million to €2,631 million quarter-on-quarter, with all segments contributing to the 6 percent growth despite the weaker US dollar. Revenue grew particularly strongly in the Automotive (ATV) segment. The Industrial Power Control (IPC) and Power & Sensor Systems (PSS) segments also recorded marked increases, while the Connected Secure Systems (CSS) saw a slight improvement compared to the previous quarter.

Revenues of the ATV segment during the three-month period rose from € 1,045 million to € 1,150 million quarter-on-quarter, with all lines of business contributing to the 10 percent growth. Demand for components for electric vehicles was particularly brisk. IPC segment revenue rose from €349 million to €362 million, up 4 percent quarter-on-quarter on the back of greater demand for renewables and home appliances. Revenue remained at a similar level for industrial drives and decreased in transportation and power infrastructure. PSS segment revenue grew by 3 percent to €779 million in the first quarter, up from €759 million in the preceding three-month period. Revenue from sensors increased significantly, while demand for power semiconductors for server, PCs and laptops remained stable on a high level.

"Infineon has made a good start to the new fiscal year. Despite headwinds from a weak US dollar, we recorded significant increases in both revenue and earnings in the first quarter. In addition to the economic recovery in some regions, we continue to benefit from the digitalization push affecting all areas of life. Semiconductors are needed more than ever," said CEO Dr. Reinhard Ploss. "We are monitoring ongoing risks closely. Nevertheless, in view of dynamic ordering momentum and manufacturing plants running at good utilization rates in the majority of product areas, we are making a slight upward adjustment to our outlook for the full year. We are increasing our investments in manufacturing capacity and bringing forward the starting date for the new power semiconductor plant in Villach to the last quarter of the current fiscal year."

"We continue to benefit from the digitalization push affecting all areas of life. Semiconductors are needed more than ever," commented Infineon's CEO Dr. Reinhard Ploss the first quarter results 2021

Based on an assumed exchange rate of $1.20 to the euro, Infineon expects to generate revenue between €2.5 billion and €2.8 billion in the second quarter of the 2021 fiscal year. Revenue generated by the ATV and PSS segments is predicted to grow by a low-single digit percentage compared to the previous quarter. Revenue in IPC is expected to remain at a similar level to the previous quarter while revenue of the CSS segment should see a low-single digit percentage declinequarter-on-quarter. For the full FY revenue of around € 10.8billion (plus or minus 5 percent) is expected. Particularly for the ATV and PSS segments, revenue is expected to grow during the second half of the fiscal year, driven by continued market momentum. "Besides geopolitical and macroeconomic factors, the economic disruption caused by the coronavirus pandemic makes accurate prediction difficult. Key factors influencing the expected development of revenue and earnings during the pandemic will be the progression of global infection rates over time, possible restrictions on economic activities, effects on production and supply chains and the level and effectiveness of governmental stimulus programs", Ploss concluded.

www.infineon.com

EPC eGaN Gate Acceleration Reliability Testing

eGaN devices have been in volume production for more than a decade and have demonstrated very high reliability in both laboratory testing and customer applications. Field reliability data over a period of four years and 226 billion hours of operation, most of which are on vehicles or used in telecommunication base stations, demonstrate a robustness that is unmatched by silicon power devices. EPC developed a custom system to assess eGaN reliability over long-term ultra-high dv/dt and di/dt pulse stress conditions such as might be encountered in automotive lidar systems. As of January 2021, devices have passed thirteen trillion pulses (about triple a typical automotive lifetime) without failure or significant parametric drift.

This Phase 12 reliability report adds to the extensive knowledge base published in the first eleven reports. It details how by employing a test to fail methodology, intrinsic failure mechanisms can be identified and used to develop physics-based models to accurately project the safe operating life of a product over a more general set of operating conditions. This methodology is also employed to consistently produce more robust, higher performance, and lower cost products for power conversion applications.

Test-to-fail vs qualification testing

Standard qualification testing for semiconductors typically involves stressing devices at or near the limits specified in their datasheets for a prolonged period of time, or for a certain number of cycles. The goal of qualification testing is to have zero failures out of a relatively large group of parts tested.

This type of testing is inadequate since it only reports parts that passed a very specific test condition. By testing parts to the point of failure, an understanding of the amount of margin between the datasheet limits can be developed, and more importantly, an understanding of the intrinsic failure mechanisms can be found. By knowing the intrinsic failure mechanisms, the root cause of failure, and the behavior of the device over time, temperature, electrical or mechanical stress, the safe operating life of a product can be determined over a more general set of operating conditions.

As with all power transistors, the key stress conditions involve voltage, current, temperature, and humidity, as well as various mechanical stresses. There are, however, many ways of applying these stress conditions. For example, voltage stress on a GaN FET can be applied from the gate terminal to the source terminal (V_{GS}), as well as from the drain terminal to the source terminal (V_{DS}). These stresses can be applied continuously as a DC bias, they can be cycled on-and-off, or they can be applied as high-speed pulses. Current stress can be applied as a continuous DC current, or as a pulsed current. Thermal stresses can be applied continuously by operating devices at a predetermined temperature extreme for a period of time, or temperature can be cycled in a variety of ways.

By stressing devices with each of these conditions to the point of generating a significant number of failures, an understanding of the primary intrinsic failure mechanisms for the devices under test can be determined. To generate failures in a reasonable amount of time, the stress conditions typically need to significantly exceed the datasheet limits of the product. Care needs to be taken to make certain the excess stress condition does not induce a failure mechanism that would never be encountered during normal operation. To make certain this is not the case, the failed parts need to be carefully analyzed to determine the root cause of their failure.

Only by verifying the root cause can a true understanding of the behavior of a device under a wide range of stress conditions be developed. It should be noted that, as more understanding of intrinsic failure modes in eGaN devices is gained, two facts have become clear; (1) eGaN devices are more robust that Si-based MOSFETs, and (2) MOSFET intrinsic failure models are not valid when predicting eGaN device lifetime under extreme or long-term electrical stress conditions.

Stress on the Gate

Figure 1 is an example of a Weibull plot of gate failures in an EPC2212 FET. The horizontal axis shows the time to failure. The vertical axis shows

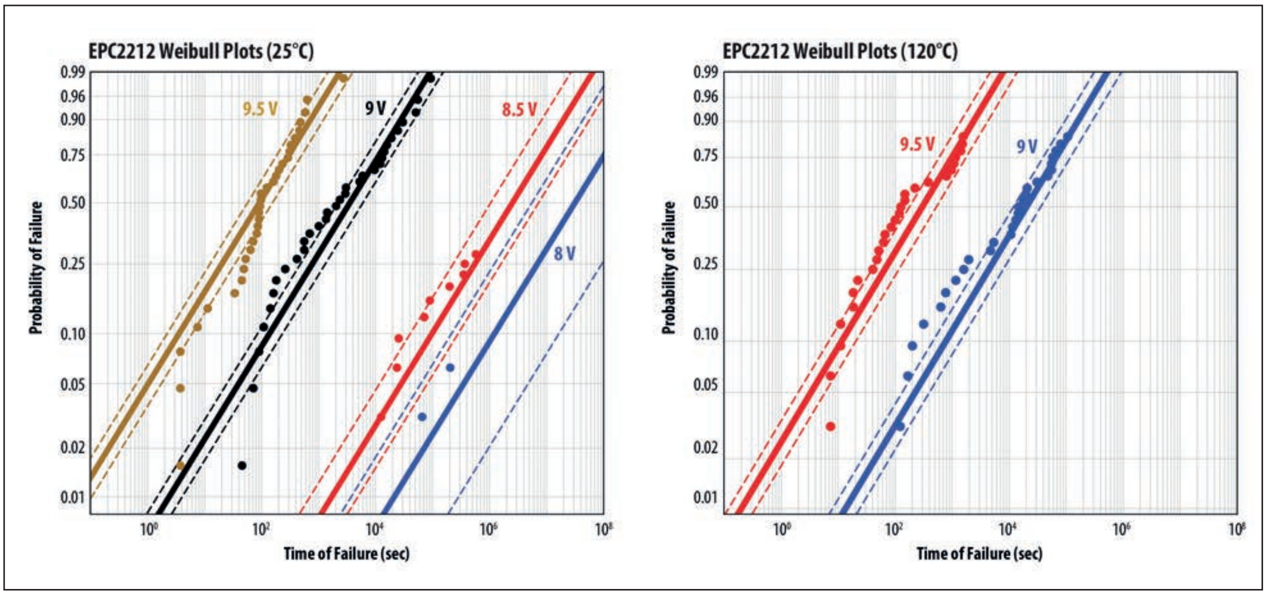

Figure 1: Weibull plots of gate-to-source failures of EPC2212. Very few failures occur even at 8 V_{GS}, yet the device has a maximum V_{GS} rating of 6 V. The data on the top is at 25°C and the data on the bottom is at 120°C

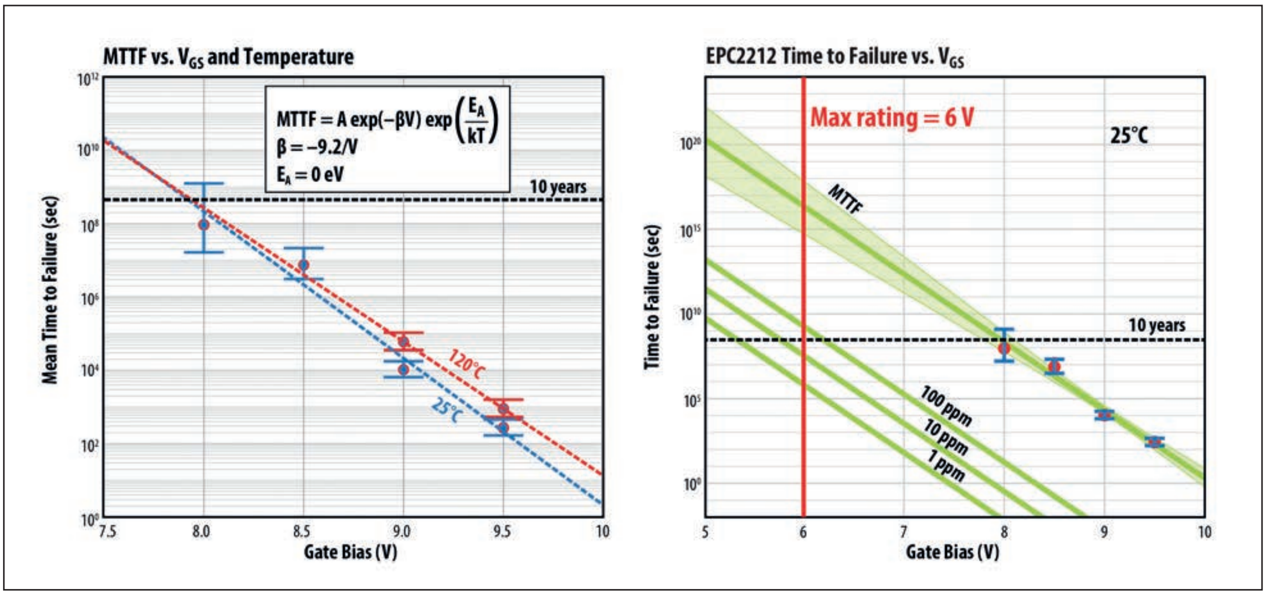

Figure 2: Mean time to failure (MTTF) for EPC2212 eGaN FETs (left) versus V_{GS} at both 25°C and 120°C. Various probabilities of failure versus V_{GS} at 25°C (right)

the cumulative failure probability for different stress conditions applied to the gate. The plot on the left has different voltages at room temperature and the plot on the right shows two different voltages applied at 120°C. This device has a datasheet maximum gate voltage rating of 6 V, yet very few devices are failing even after many hours at 8 V.

In Figure 2 these data have been translated into failure rates. On the left is the mean time to failure (MTTF) for these same devices vs V_{GS} at both 25°C and 120°C. On the right is a graph that shows the various probabilities of failure versus V_{GS} at 25°C. The failure rate is not very sensitive to temperature but is very sensitive to V_{GS}.

Looking at the graph on the right, with a V_{GS} of 6 V DC, which is the absolute maximum allowed voltage for this part one could expect between 10 and 100 parts per million (ppm) failures in 10 years. The recommended gate drive voltage, however, is 5.25 V and the expected failure rate at that voltage is less than 1 ppm in 10 years.

These conclusions are only valid if the primary failure mechanism is the same under all these conditions. In order to confirm this, failure analysis was performed on multiple parts from this study, and a consistent failure mode was found. Referring to the image in Figure 3, the yellow circle indicates the failure site is between the gate metal and the metal 1 layer. These two layers are separated by a Silicon Nitride dielectric layer. It is this layer that failed, not any of the GaN layers beneath.

While this lifetime study provided a solid phenomenological model of gate reliability in eGaN FETs, many fundamental questions remained unanswered:

- Is the exponential scaling of MTTF with gate voltage truly applicable to eGaN FETs? Is there perhaps a different mathematical model that is predicated on the root physics of failure in GaN?
- Why does dielectric rupture occur in a high-quality silicon nitride film at an electric field well below its breakdown strength? And, why does this rupture occur at the corner of the gate?
- Why does gate lifetime increase as temperature rises?

To resolve these questions, EPC conducted more extensive gate acceleration studies on recent lots of EPC2212 devices, using larger sample sizes and longer durations (> 1000 hours in some cases). In addition, several core experiments to uncover the dynamics of failure at high gate bias were performed. These studies resulted in an improved understanding of the physics of failure and, for the first time, a lifetime equation specific to eGaN technology that is derived directly from this physics.

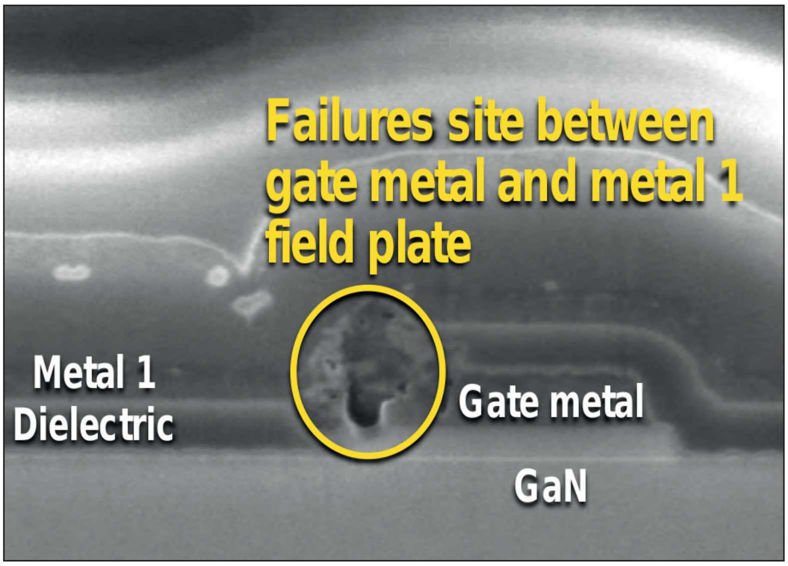

Figure 3: Scanning electron microscopy (SEM) image of the gate region of an EPC2212 eGaN FET. The yellow circle shows the failure site is between the gate metal and the metal 1 layer

EPC has gathered convincing evidence that gate failure at high bias in eGaN FETs is caused by a two-step process. In the first step, impact ionization inside the p-GaN gate layer leads to the production of electron-hole pairs. Some of these holes scatter and trap in the Si3N4 layer near the corner(s) of the gate. Over time, as this trapped hole charge density accumulates, the electric fields in the dielectric grow until, at a certain critical charge density, it ruptures catastrophically.

Figure 4 shows the lifetime model plotted against the measured MTTF of an EPC2212 eGaN FET from a recent acceleration study. In contrast with the simple exponential model, the new equation bends upward at low gate bias, resulting in an increased life expectancy when the devices are operated within their datasheet range (< 6 V). In addition, the new model provides a better fit to measurement, wherein the voltage acceleration is observed to decrease as VGS rises. Figure 5 shows the temperature dependence of the lifetime equation at ?75°C, 25°C, and 125°C. At higher temperature the MTTF is slightly higher, as observed in the measurements shown in Figure 2.

Safe Operating Area Testing

Safe operating area (SOA) testing exposes the eGaN FET to simultaneous high current (I_D) and high voltage (V_{DS}) for a specified pulse duration. The primary purpose is to verify the FET can be operated without failure at every point (I_D, V_{DS}) within the datasheet SOA graph. It is also used to probe the safety margins by testing to fail outside the safe zone.

During SOA tests, the high-power dissipation

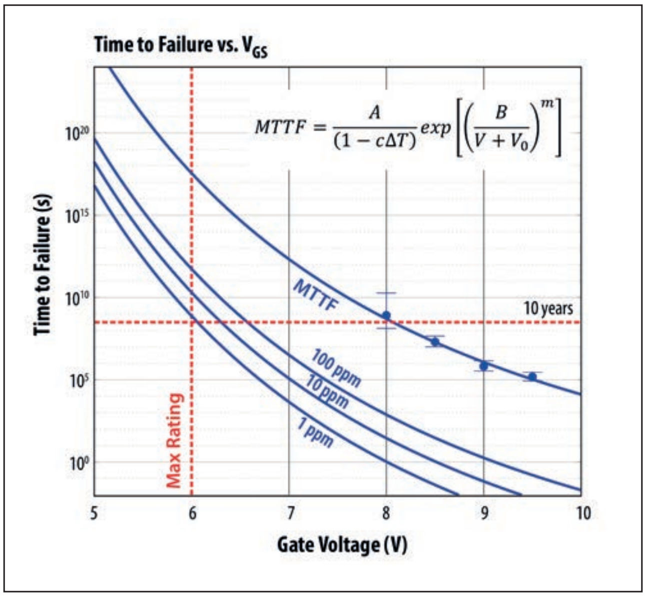

Figure 4: EPC2212 MTTF vs. V_{GS} at 25°C MTTF (and error bars) are shown for four different voltage legs. The solid line corresponds to the impact ionization lifetime model. Extrapolations of time to failure for 100 ppm, 10 ppm, and 1 ppm are shown as well

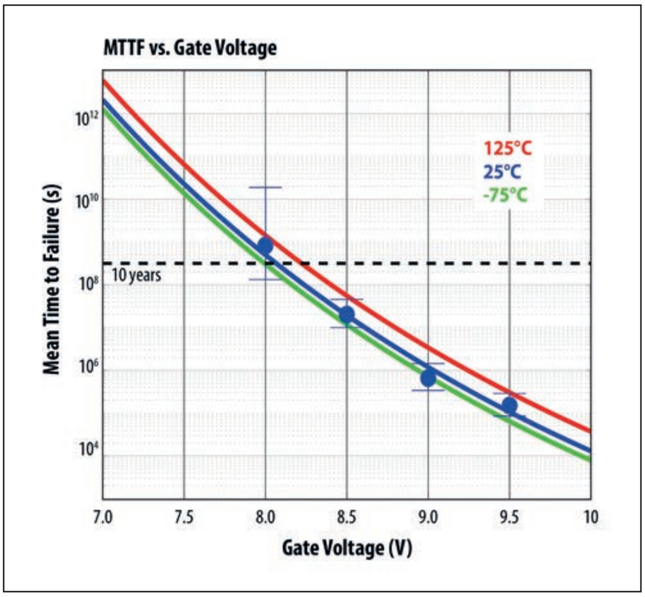

Figure 5: Measured MTTF for EPC2212 (25°C) measured at four different gate biases. Blue line is lifetime model. Red and green lines are predictions of the lifetime model at 125°C and ?75°C respectively

within the die leads to a rapid rise in junction temperature and the formation of strong thermal gradients. For sufficiently high power or pulse duration, the device simply overheats and fails catastrophically. This is known as thermal overload failure.

In Si MOSFETs, another failure mechanism known as secondary breakdown (or Spirito effect) has been observed in SOA testing. This failure mode, which occurs at high VD and low ID, is caused by an unstable feedback between junction temperature and threshold VTH. As the junction temperature rises during a pulse, VTH drops, which can cause pulse current to rise. The rising current, in turn, causes temperature to rise faster, thereby completing a positive feedback loop that leads to thermal runaway and ultimate failure. A goal of this study is to determine if the Spirito effect exists in eGaN FETs.

EPC designed and built a custom SOA test system which works similar to a curve tracer. The gate bias on the device under test (DUT) is set before the pulse and is used to modulate the ultimate pulse current. The drain voltage is then pulsed onto the drain by means of a p-channel control FET for a specified pulse duration.

For DC, or long-duration pulses, the SOA capability of the FET is highly dependent on the heatsinking of the device. This can present a huge technical challenge to assess the true SOA capability, often requiring specialty water-cooled heatsinks. However, for short pulses (< 1 ms), the heatsinking does not impact SOA performance. This is because on short timescales, the heat generated in the junction does not have sufficient time to diffuse to any external heatsink. Instead, all of the electrical power is converted to raising the temperature (thermal capacitance) of the GaN film and nearby Silicon substrate. As a result of these considerations, SOA tests were conducted at two pulse durations - 1 ms and 100 µs.

Figure 6 shows the SOA data of 200 V EPC2034C. In this plot, individual pulse tests are represented by points in (I_D, V_{DS}) space. These points are overlaid on the datasheet SOA graph. Data for both 100 µs and 1 ms pulses data are shown together. Green dots correspond to 100 ?s pulses in which a part passed, whereas red dots indicate where a part failed. A broad area of the SOA was interrogated without any failures (all green dots), ranging from low V_{DS} all the way to $V_{DS(max)}$ (200 V). All failures (red dots) occurred outside the SOA, indicated by the green line in the datasheet graph. The same applies to 1 ms pulse data (purple and red triangles); all failures occurred outside of the datasheet SOA.

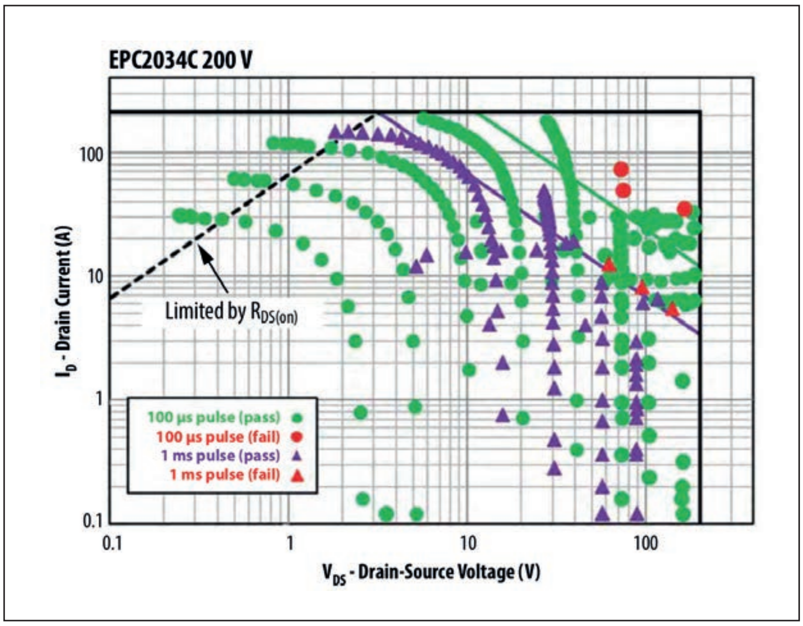

Figure 6: EPC2034C SOA plot. The "Limited by RDS(on)" line is based on data sheet maximum specification for $R_{DS(on)}$ at 150°C. Measurements for 1 ms (purple triangles) and 100 µs (green dots) pulses are shown together. Failures are denoted by red triangles (1 ms) or red dot (100 µs). Note that all failures occur outside the data sheet SOA region

Literature

EPC Reliability Report - Phase 12: Alejandro Pozo, Shengke Zhang, Gordon Stecklein, Ricardo Garcia, John Glaser, Zhikai Tang and Robert Strittmatter, Efficient Power Conversion Corporation

www.epc-co.com

Yokogawa Launches NextGen ScopeCorder

Yokogawa Test & Measurement has added in March another new instrument to its ScopeCorder family of portable multi-channel data-acquisition recorders, extending and improving their speed, channel count and data acquisition features. The DL950 is designed to offer a highly detailed view of an application's electrical and mechanical behavior.

"With the DL950, the ScopeCorder family attains new levels of data acquisition speed and greatly improved usability", says Terry Marrinan, Yokogawa Test & Measurement's Vice President for Europe & South East Asia. "Offering the versatility to discover more from a large number of input types, the insight available from a high bit resolution and a high level usability from easy set-up, the DL950 gives developers the tools they need to gain detailed information on the behavior of energy efficient and new renewable energy technologies and devices."

The new ScopeCorder is inteded for many markets, including transportation for applications such as testing electric vehicles and also associated SiC/GaN inverters. For power and harmonics analysis the G05 option is available. Here a single DL950 can evaluate a system with battery-driven motors, such as an EV. The DL950 calculates the conversion efficiency from the input and output power of the inverter and analyzes the effects of harmonics caused by external disturbances while capturing mechanical variations in motor speed and torque. Uses in the power and energy sector include capturing data on renewable energy systems, while in industrial equipment it can be used for testing high efficiency motors, robots and sensors (Figure 1).

Oscilloscope and recorder with large touch screen

The DL950 is easy to use via a large 12.1 inch touch screen, providing convenient access to its features. Yokogawa's power analyzers and a selection of other instruments can be time synchronized through the device's integrated IEEE1588 PTP master function and the IS8000 Integrated Software Platform. The units can also be controlled remotely, allowing home workers to continue conducting tests while working away from the test laboratory. Dedicated application menus simplify the setup. Touching an application icon brings up the graphical setup screen for the application, while users can also register frequently used applications as favorites.

Providing a combination of high-speed sampling and signal fidelity of an oscilloscope and the long-term data recording capabilities of a recorder, the DL950 measures signals at a high bit resolution while securing data in harsh environments. Building on the capabilities of the DL850E, the new DL950 ScopeCorder can handle larger amounts of data at a faster sample rate and with a longer recording time. It has a large acquisition memory up to 8 Gpoint, and a 200 MS/s sample rate at 14-bit, compared to the DL850E's 100 MS/s at 12-bit. Up to 32 isolated analog channels with 10 MS/s at 16-bit or up to 128 digital

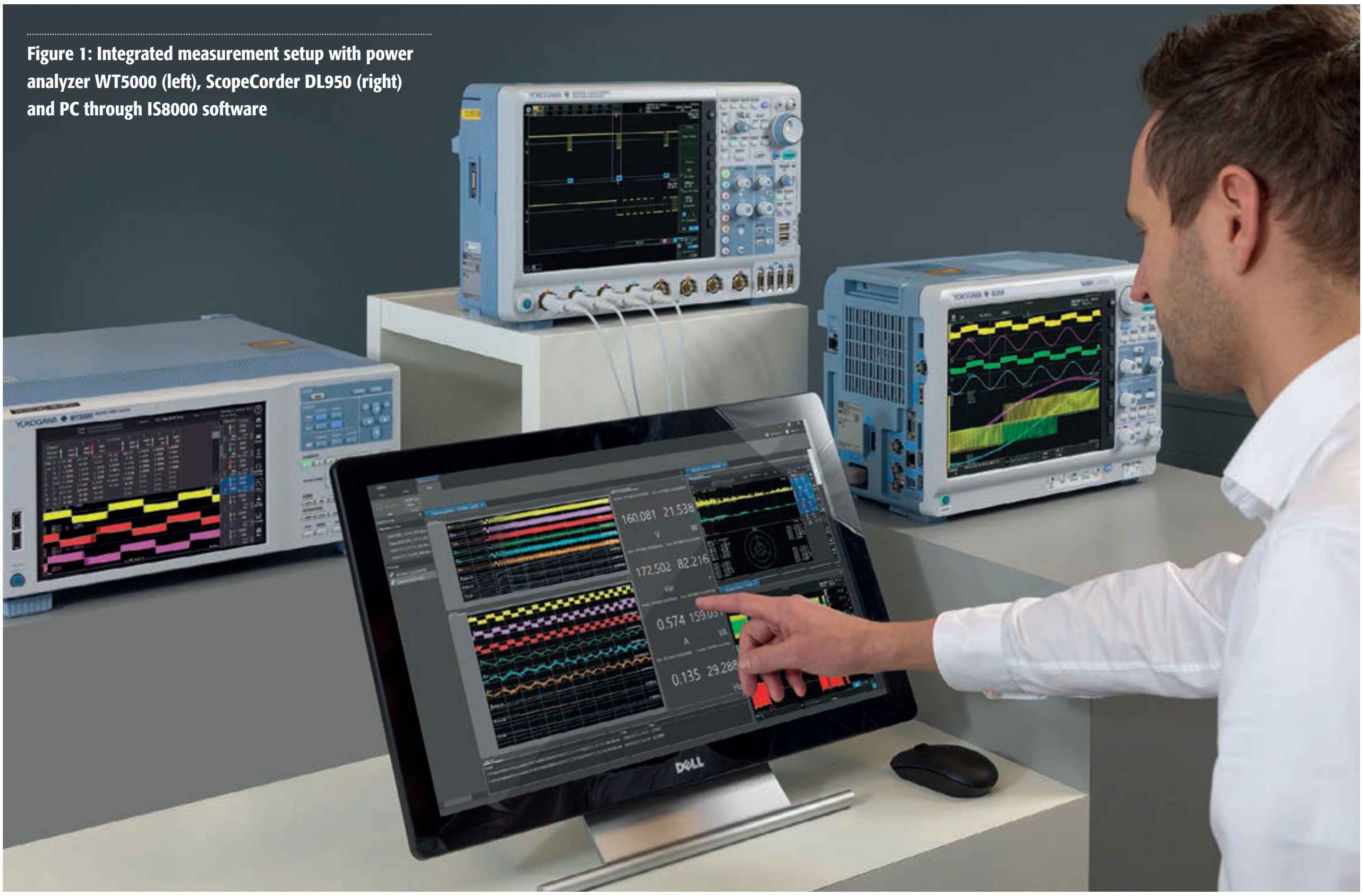

Figure 1: Integrated measurement setup with power analyzer WT5000 (left), ScopeCorder DL950 (right) and PC through IS8000 software

channels can be provided.

The dual capture feature offers both data acquisition recorder functionality and the sample speed and trigger features of an oscilloscope. This allows developers to analyze the finest waveform details while observing multi-channel measurements over longer periods. Five options for acquiring data, allowing users to choose the best method for their application are offered. They can opt for normal acquisition into the fast internal acquisition memory, recording to flash memory (coming soon), recording to the internal hard disk (SSD) or directly to the PC via normal Ethernet or opt for 10 Gigabit Ethernet. Data can be captured to a PC streaming over a very long time at up to 160 MB/s, with data volumes limited only by the PC's storage. Using 10 Gigabit Ethernet, data can be transferred from the DL950 to a PC at 50 times the speed of its predecessor. A fiber optic cord and the Yokogawa's IS8000 PC software are used for transmission. The DL950 will also feature Flash Acquisition (coming soon), used to store data when a PC cannot be used, for example when capturing data from within a vehicle, power plant or other similar applications. In this case data can be captured over a long time with a high-speed sample rate of 20 MS/s (8 CH) and 10 MS/s (16 CH).

The 512 GB internal SSD can record up to 50 days. Depending on the sample rate it can record for five hours on one channel at up to 2 MS/s, or record at 200 kS/s for 20 hours with 16 channels. Waveforms from dual capture can also be recorded, useful for in-vehicle endurance testing and capturing rare spontaneous events.

21 types of input modules are available, including 12-, 14- and 16-bit isolation modules, universal voltage/temperature modules, acceleration/voltage modules, strain modules and frequency modules.

Up to five DL950s can be synchronized to allow the use of up to 160 voltage channels. Alternatively, up to 640 temperature channels can be used, employing 16 channels with eight slots for each of five DL950 units. The subunits can be synchronized to start and stop their measurements via signals from the main unit. Following a few typical applications where the DL950 can be used.

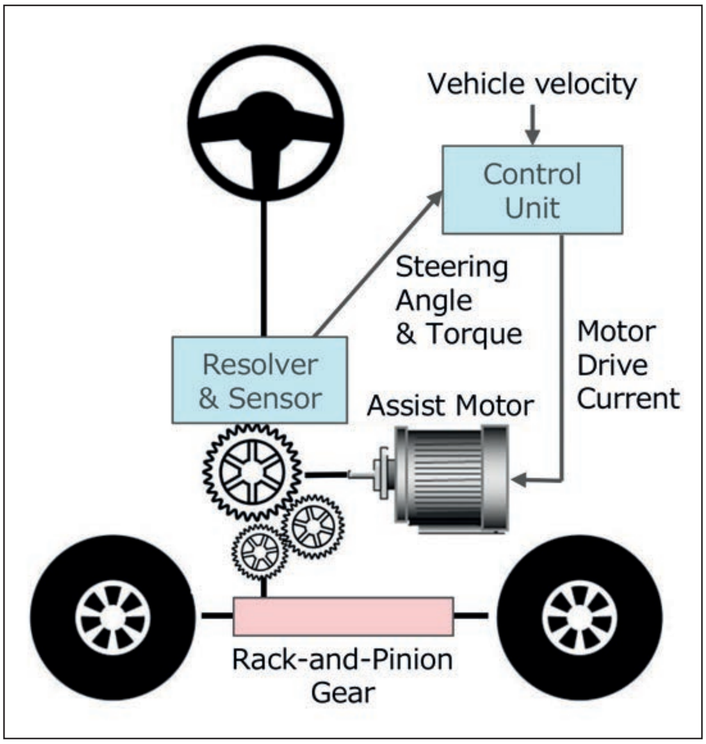

Figure 3: In power steering application the DL950 can simultaneously record voltage, current, and CAN data Yokogawa-EPS.JPG

Application SMPS output monitoring

There are many tests needed for SMPS design such as power quality, inrush current, and MOSFET switching testing (Figure 2). One of the key tests is to monitor and record the SMPS output current characteristics when connected to different loads at a high sampling rate for a long period of time. Any change in output current due to the dynamic load conditions is monitored and saved for further analysis. To perform this test, engineers need an instrument that can meet the requirements of SMPS output voltage and current measurement, isolated input channels, high A/D resolution, high speed data sampling rate, long period of recording time (a few minutes to an hour), and data storage. For this application the 200MS/s, 2-channel- 14 bit isolated module 720212 is available. It offers a bandwidth from DC to 40 MHz ans an input voltage of 1000 V(DC+ACpeak). The 4CH 10 MS/s 16-bit isolated module 720256 offers a bandwidth from DC to 3 MHz at 600 V (DC+ACpeak).

Here the DL950 can be used as a normal oscilloscope to conduct other tests such as power quality, inrush current, and MOSFET switching testing (amplitude, duty cycle, frequency). Also, it can be used as a recorder by switching oscilloscope/recorder mode. Users can use the DL950 in a measuring instrument mode they are familiar with.

Electric power steering

Electric Power Steering (EPS) uses an electric motor rather than hydraulic pressure to assist in automobile steering (Figure 3). As the use of electronic control systems for the entire vehicle progresses, EPS systems have been introduced, resulting in lighter weight compared to hydraulic systems, which improves fuel efficiency and provides greater control flexibility by changing the steering force for each vehicle speed.

In addition to EPS, this technology improves vehicle stability by cooperating control of brakes and throttle, and supports tandem parking and garage parking by cooperating with Intelligent Parking Assist (IPA). To evaluate an EPS steering subsystem, it is necessary to continuously record and analyze the steering angle, various sensor outputs, ECU inputs and outputs, etc. in an integrated manner. The DL950 ScopeCorder provides the measurement capabilities required by

Figure 2: In SMPS testing the DL950 can be used as a normal oscilloscope to conduct other tests such as power quality, inrush current, and MOSFET switching testing

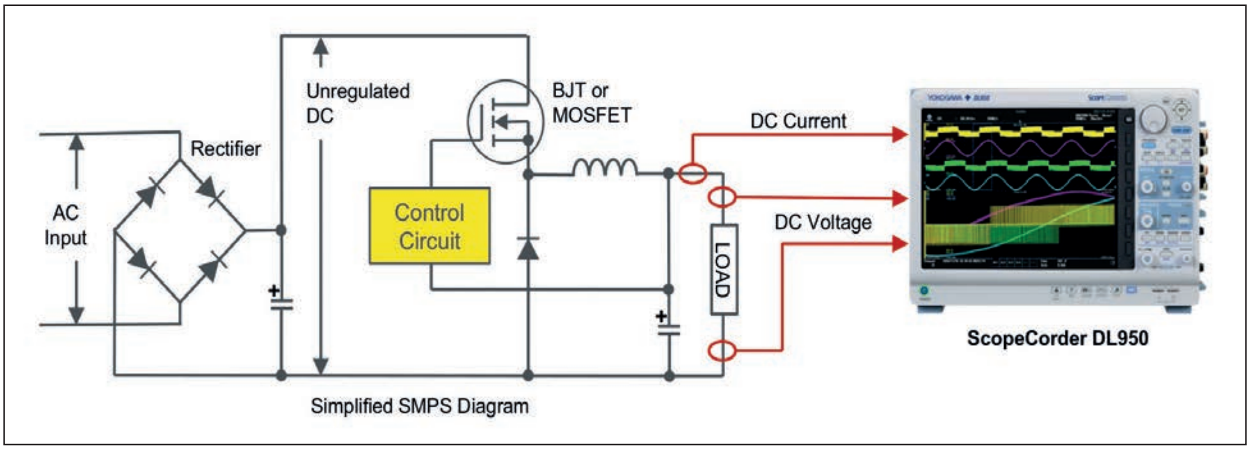

engineers designing and evaluating EPS in a single unit.

Torque generated by steering wheel operation is transmitted to torsion bar, rack and pinion gears. These forces are detected by the torque sensor and transmitted to the ECU. ECU applies current (power assist amount) to assist motor according to torque and vehicle speed. To develop and evaluate EPS systems, it is necessary to monitor and record a large number of signals, such as sensor (vehicle speed, torque, torsion, rack axial tension, battery power) signals (often voltage output via amplifier), three-phase motor current, voltage, and rotation amount, as well as power assist amount (CAN data) calculated by ECU. In addition, since continuous recording of about 10 to 20 minutes is required, long memory is also required.

The DL950 can simultaneously record voltage, current, and CAN data over a long period of time using a multi-channel, real-time calculation function to calculate and display torque and steering angle. In addition, it is possible to calculate the rotation angle of the assist motor from the encoder output, and to record vibration and sound at the same time, so that the EPS system can be evaluated in an integrated manner.

Evaluation of ECU and inverter/motor

Inverter and motor controlled by ECUs in electric vehicles (EV) require even higher levels of control and responsiveness (Figure 4). In addition to confirming the operation of the control program, it is becoming increasingly important to comprehensively measure the control program instructions and the actual operation of the inverter/motor, and to evaluate their behavior, responsiveness or validity. In order to perform these evaluations, the CAN / CAN FD data from the ECU, the battery output, the internal control and output voltage/current of the inverter, and the torque / rotation speed of the motor must be integrated and measured.

In waveform measurement of high voltage or large current, there is a possibility of short circuit, electric shock accident or damage of the measuring instrument caused by insulation failure, wrong wiring, over-input, etc. In order to prevent such accidents, it is important that the measurement instrument has an isolated input. The ScopeCorder offers a variety of isolated input modules, including up to 1000 V input modules.

Voltage and current of various motors and control systems, motor rotation speed, battery voltage fluctuation, vibration, noise, temperature, strain, etc. may be measured simultaneously. The DL950 has a maximum of 32 channels, and a 5-unit synchronization provides up to 160 channels.

High-speed sampling is required to understand sudden voltage fluctuations in inverters and batteries. The DL950 is capable of sampling up to 200 MS/s. You can also set a different sample rate for each channel, reducing the amount of data combined with slower sample channels such as temperature.

The in-vehicle serial bus data of CAN / CAN FD, LIN, SENT can be displayed by trend. For example, vehicle speed data on CAN FD can be measured simultaneously with sensor outputs such as voltage and current of motor drive, motor speed, temperature and vibration.

The CAN/CAN FD bus data and related waveforms can be viewed on the same screen. For example, an ignition switch ON/OFF signal, a CAN FD signal corresponding to that command, and pressure signals can be checked on the same screen to verify the correlation between them.

Synchronous measurements

A motor/inverter evaluation bench system incorporates equipment such as a power meter and a waveform measurement instrument. Generally, when acquiring the evaluation data, it is necessary to collect data from each instrument, and, commonly, a data collection system is designed. For example, a power meter obtains measured data including DC voltage, DC current, and DC power that are input from a battery to an inverter, and three-phase AC voltage, AC current, active power, frequency, and power factor that are output from the inverter to a motor—all at a data update rate of one second. A waveform measurement instrument such as an oscilloscope performs high-speed data acquisition at 1 or 10 MS/s to capture the carrier frequency of the inverter more accurately. It saves both power data and waveform data as a series of evaluation data to create a report that is based on the evaluation results.

Power data may be transferred and saved to a PC from a power meter at a data update rate of one second or 100 ms. Since the size of a single item of numerical data is about four bytes, the data volume is small and the data transfer time is unlikely to be a problem even when acquiring 32 items of data, such as inverter input/output voltage, current or power, by a PC. On the other hand, when three-phase inverter waveforms are transferred and saved to a PC from a waveform measurement instrument at a sample rate of 10 MS/s, there are six waveforms of voltage and current signals and it is necessary to transfer a large amount of data, 60 MB/s. Where the amount of waveform data is too large to transfer to a PC within a given time, the data may be saved in the waveform measurement instrument and transferred to the PC after the measurement to continue an evaluation test. However, the data transfer may take several minutes instead of several seconds, during which the evaluation test is interrupted.

Since the data is acquired from the power meter and the waveform measurement instrument separately, it is necessary, at least, to match the

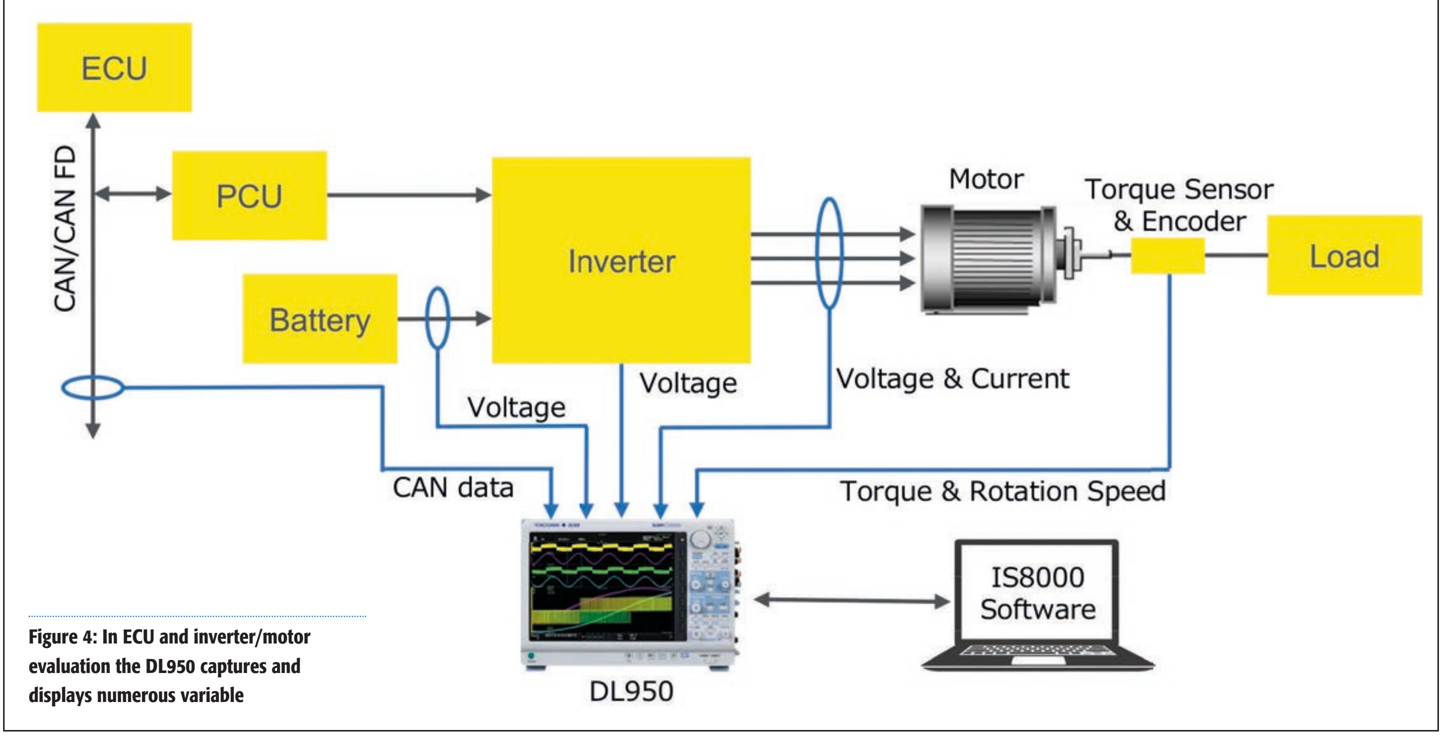

Figure 4: In ECU and inverter/motor evaluation the DL950 captures and displays numerous variable

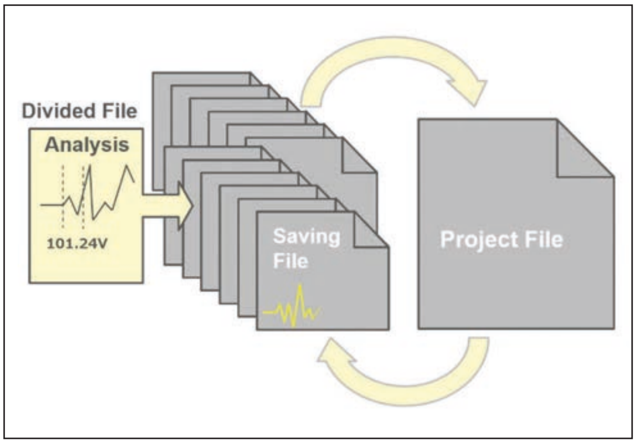

Figure 5: Integrating a project file and divided files

start time of the observation on that instrument with the start time on the power meter (the position of the data update cycle) to time-synchronize the waveform sample rate with the power values or calculated values of the power meter. It is practical to synchronize the times in units of one second, but it is quite difficult to manually perform time synchronization within 100 ms. Now, since more tests require the simultaneous acquisition of waveform data and power data, ensuring the simultaneity of data has become a major issue.

With the 10G Ethernet interface option (/C60), the DL950 provides 10 Gbps high-speed data transfer. While the conventional model DL850E provides PC streaming at 100 kS/s (16ch), the DL950 offers 50 times faster data transfer at 10 MS/s (8ch), allowing measured data to be displayed on the PC software in real time. In inverter measurement, the high switching frequency requires high-speed data capture.

The DL950 transfers data continuously to a PC at up to 10 MS/s, so that the data can be output without interrupting the test. There is no need to wait a matter of minutes just for data transfer to complete. Furthermore, by combining the ScopeCorder DL950 with the WT5000 power analyzer, it is possible to achieve an industry first by performing high-precision power measurement with power traceability in synchronization with high-speed waveform data.

The IS8000 integrated measurement platform can manage individual files as one project file. This eliminates the need to save a waveform data file and a power data file with the same name to associate them with each other or the need to manage files by creating a folder for each measurement data and storing a waveform file and a power data file in that folder. A data file can be divided into segments by specifying the length of time. The data for an entire measurement period and the data for the period desired for analysis during the measurement can be saved as separate files.

For example, when measuring for 24 hours, the user can divide the file into one-hour segments and analyze the data of the segments where the measuring process is finished while continuing the measurement. After the measurement is completed, the file of the entire measurement period and the divided files can be managed as a project file. Measurement using two DL950s or measurement using the DL950 and WT5000 can also be managed as one project file. The fact that the user does not have to associate file names even in the measurement with the DL950 and WT5000 supports the improvement of development efficiency.

The automatic report creation option (/RP1) allows report creation and output on a PC. A report can easily be created by setting the report layout (with image display) using the report creation wizard function (Figure 5). From the files measured or saved by the ScopeCorder or the Precision Power Analyzer, the user can choose measurement conditions, waveform output, measurement results, or other data. The report can be output to PDF or EXCEL.

https://tmi.yokogawa.com

New Developments in RET Technology

Resistor-Equipped Transistors (RETs) – also known as digital transistors or pre-bias transistors – offer many benefits, including saving space, reducing manufacturing costs and increased reliability. This article looks at their structure and design considerations, and considers the suitability of new, 80 V parts that target emerging 48 V EV systems. **Burkhard Laue, Application Marketing Manager and Reza Behtash, Application Marketing Manager at Nexperia Europe**

Bipolar transistors are controlled using the base current. However, because the voltage drop across the base-emitter path is highly temperature-dependent, in most applications a series resistor is required to keep the base current at the desired level, thereby ensuring the stable and safe operation of the transistor. To reduce the component count and to simplify board designs, RETs combine single or dual bipolar transistors with the bias resistors which are integrated on the same die. Because these internal resistors have higher tolerances than commonly used external resistors, RETs are suitable for switching applications where the transistor operates in either on- or off-state. This is why RETs are often referred to as digital transistors. RETs are available in many voltage, current and resistance values, in NPN or PNP configuration and a variety of packages including SOT23 and SOT323 and SOT363.

Bipolars for automotive applications

Two common forms of RETs are shown in Figure 1. In Figure 1a, two resistors and a transistor are integrated with a single NPN transistor. The base series resistor is labeled R1 and a second resistor, R2, in parallel to the base-emitter path completes the base divider circuit. The base divider provides fine tuning and better turn-off characteristic behavior. Nexperia offers R1 values from 2.2 kΩ to 47 kΩ and R2 values from 10 kΩ to 47 kΩ. The ratio of the resistors R2/R1 can be 1, 2.13, 4.55, 10 and 21. Figure 1b shows a dual version with two transistors and four resistors.

The RET structure is very similar to the well-understood, standard BJT. Figure 2 shows the resistance 'meander' created using a standard device processing step where a polysilicon layer is deposited on the die and then etched back, structured and patterned to form the integrated resistor layer. Figure 3 shows a cross section of a 100 mA automotive RET.

Nexperia offers two types of RETs: so-called performance-based 600 mA 40 V RETs; and standard devices which are available as 50 V devices and 80 V parts which have recently been uprated, primarily to cope with new 48 V automotive systems.

The 600 mA RETs are based on the company's performance-based, low VC saturation BJTs that have a good current amplification. This gain stays high at high-collector currents, which is very important because less base energy is required, so the transistor can more easily be turned

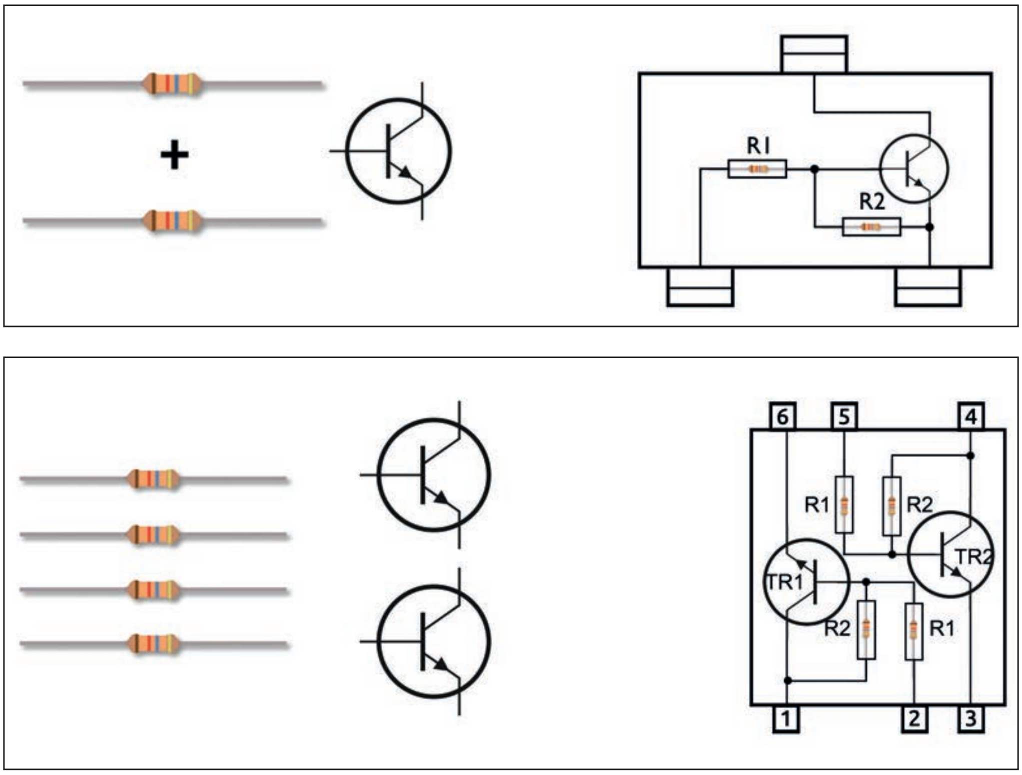

Figure 1: Two common forms of RETs, two resistors and a transistor are integrated with a single NPN transistor (a), dual version with two transistors and four resistors (b)


TARGET YOUR BUYERS
FROM OVER 60,000
QUALIFIED CONTACTS
E-CAMPAIGN
LIST RENTAL
LEASE
DfA media
Direct
Contact: Ian Atkinson
on +44 (0)1732 370340
ian.atkinson@dfamedia.co.uk
SMART MACHINES & FACTORIES
PWE Plant & Works Engineering
Drives&Controls
POWER ELECTRONICS EUROPE
Hydraulics&Pneumatics
THE JOURNAL OF FLUID POWER AND SYSTEMS

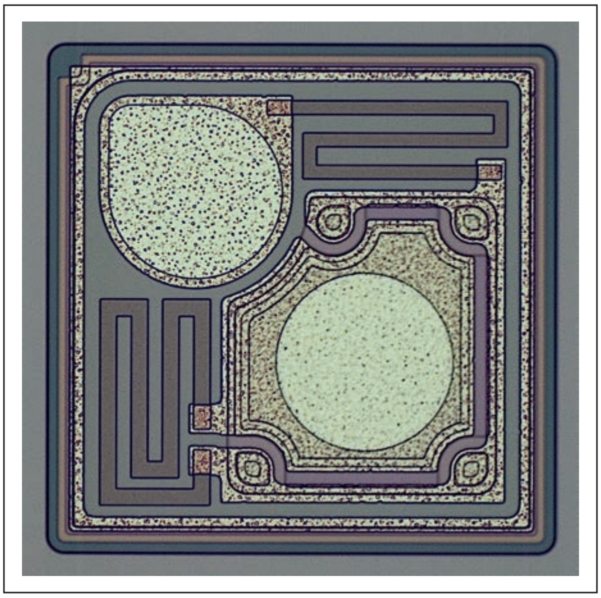

Figure 2: Resistance 'meander' created using a standard device processing step

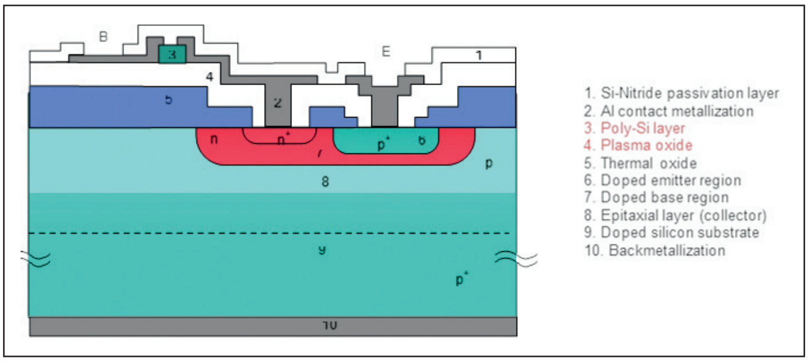

Below Figure 3: Cross section of a 100 mA automotive RET

on, even at high load currents. Also, the residual voltage across this switch and the on status is lower compared to a standard transistor, so overall they achieve a much better power efficiency. Dies size can also be reduced.

In use it is important that as little heat is generated in the load path transistor, so again, it is useful if the transistor has a good current amplification (h_{FE}), which does not degrade and improves with temperature over the load current. As an example, Figure 4 shows the performance of PBRN113ZT 600 mA, 40 V R1/RT2 1 kΩ/10 kΩ NPN performance-based RETs.

Another benefit of the technology is the relative tight tolerance of the R1/R2 ratio of the integrated resistors for RETs with current values above 100 mA, which at +/-10% are three times more accurate than other products. This enables the input voltage safety margin to be reduced.

Design considerations

While RETs offer many significant benefits, some important design considerations should be noted. Figure 5 shows the switching characteristic of a RET plotting V_{CE} versus V_i. $V_{i(off)}$ is the input voltage the RET turns off. The condition required for an off-state is that the collector leakage current must be 100 μA at a collector-emitter voltage of 5 V. For safe turn-off, $V_{(ioff)max}$ must not be exceeded. When determining the on-state, $V_{i(on)min}$ must be considered. The circuit controlling the RET has to provide at least this voltage for a safe turn. On-state is defined as a collector current of 10 mA while the collector-emitter voltage is 0.3 V. The datasheet V_i rating is valid for the test condition defined only. If a bigger collector current shall be switched the RET requires more base drive voltage Vi(on):

$V_i < V_{i(off)max}$ - a RET is in off-state for every device shipped

$V_i < V_{i(off)typ}$ - a typical RET is in off-state

$V_i > V_{i(on)typ}$ - a typical RET is in on-state

$V_i > V_{i(on)min}$ - a RET is in on-state for every device shipped.

It is also important to consider the same diagram at different temperature ranges. BJT switches become more effective as the temperature goes up, so they will safely stay on if temperature becomes higher. That's fine, for example, in an autonomous vehicle application in a hot climate; however, if you drive in a cold climate you have to be careful that the BJT stays in on-state, because at low temperatures the BJT gain goes down and the BJT current gain goes down and the voltage drop V_{BE} increases, so a higher turn-on voltage is required.

Table 1 shows the dependency of the on- and off-state input voltages on the resistor divider configuration in RETs from NHDTC series RETs.

The selection of a proper resistor divider option is also important to ensure that the control voltage window of the RET matches the driving stage.

New 80 V automotive RETs

BJTs are preferred in many automotive applications due to their robustness.

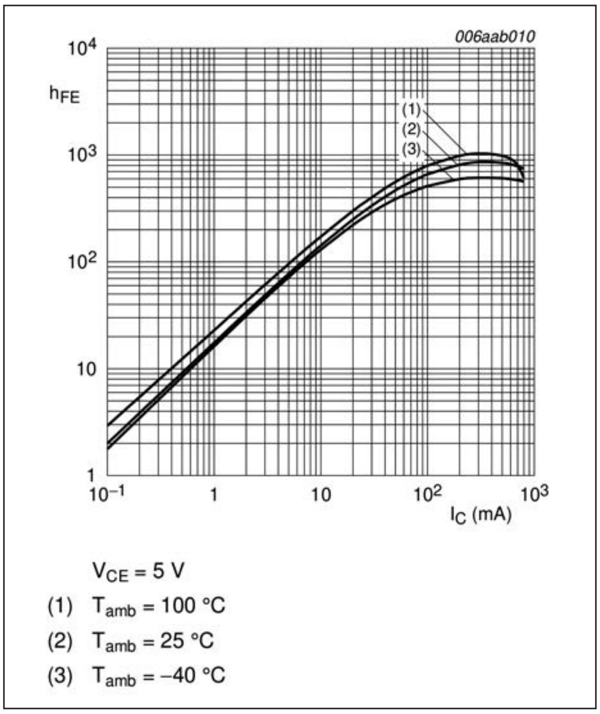

Figure 4: Performance of PBRN113ZT 600 mA, 40 V R1/RT2 1 kΩ/10 kΩ NPN RET

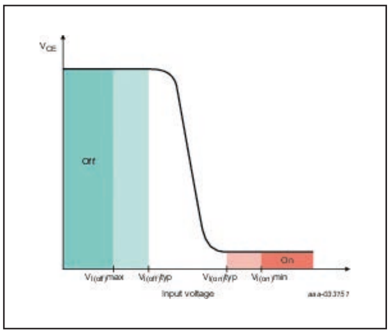

Figure 5: Switching characteristic of a RET

Nexperia's standard 50 V RETs are to be found in very many automotive applications. One typical application is converting from a low voltage, such as 3-3.3 V for a microcontroller to the battery voltage of 12 V. Now, with the introduction of 80 V parts, they are suitable for 48 V e-vehicles and hybrid applications.

RETs provide a simple way to switch and drive loads directly from logic devices. Some example circuits are shown in Figure 6. This has not been too challenging for RETs when the battery voltage V_{cc} is 12 V. However, with the uptake in electric vehicles with a 48 V board net, much more headroom has become necessary. Nexperia's 80 V RETs provide the safe operating margin required.

There is another driver. Automotive customers are now demanding that devices meet pulse tests in accordance with ISO 7637-2:2011, the standard that defines robustness against transients along the power supply bus. At the behest of a major Tier 1 supplier to the EV industry, Nexperia's 80 V RETs have been tested and withstand the required 20 V across base-emitter junction. This is vital for 24 V systems in trucks and lorries, and 48 V automotive systems.

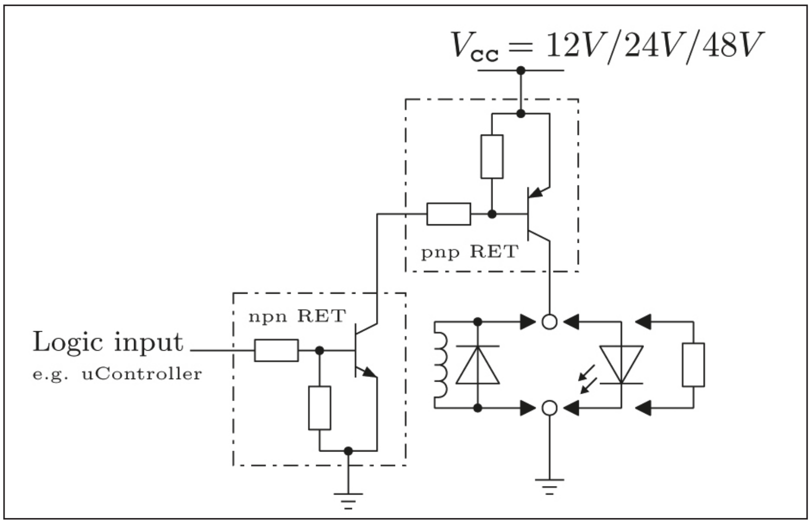

Figure 6: Example application circuits

Conclusion

Nexperia has many millions of RETs delivering safe, reliable and efficient switching in automotive and many other applications. The company's new range of AEC-Q101-certified 80 V products has the performance, robustness and efficiency required to provide safe operation in 48 V board net e-mobility applications. With the move towards autonomous vehicles, reliable switching systems are going to be required in even more automotive applications.

Below Table 1: Dependency of the on- and off-state input voltages on the resistor divider configuration

R1/R2	$V_{I(on)}$ min	$V_{I(on)}$ typ	$V_{I(off)}$ typ	$V_{I(off)}$ max	RET Type
10k/10K	2.5	1.8	1.15	0.8	NHDTC114ET
22K/22k	3	2.3	1.15	0.8	NHDTC124ET
47k/47k	5	3.3	1.15	0.8	NHDTC144ET
2.2k/47k	1.2	0.81	0.595	0.5	NHDTC123JT
4.7/47k	1.4	0.95	0.625	0.5	NHDTC114YT
10k/47k	1.6	1.22	0.690	0.5	NHDTC143ZT

Accelerated Life Test Instruments

www.accelrf.com
Accel-RF Instruments Corporation
Tel: 001 858 278 2074

Arbitrary 4-Quadrant Power Sources

www.rohrer-muenchen.de
Rohrer GmbH
Tel.: +49 (0)89 8970120

Busbars

www.auxel.com
Auxel FTG
Tel: + 33 3 20 62 95 20

Capacitors

www.cde.com
Cornell Dubilier
Tel: 001 508 996 8561

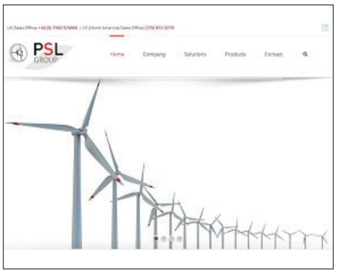

www.psl-group.uk.com
PSL Group UK Ltd.
Tel +44 (0) 1582 676800

Certification

www.productapprovals.co.uk
Product Approvals Ltd
Tel: +44 (0)1588 620192

Connectors & Terminal Blocks

www.auxel.com
Auxel FTG
Tel: +44 (0)7714 699967

Cost Recovery, Research & Development/IP

www.mcs-corporate.com
MCS Corporate Strategies Limited
Tel: 01926 512475

DC/DC Connverters

www.power.ti.com
Texas Instruments
Tel: +44 (0)1604 663399

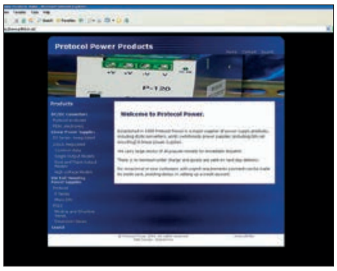

www.protocol-power.com
Protocol Power Products
Tel: +44 (0)1582 477737

Diodes

www.neutronltd.co.uk
Neutron Ltd
Tel: +44 (0)1460 242200

www.microsemi.com
Microsemi
Tel: 001 541 382 8028

Diodes

www.proton-electrotex.com/
Proton-Electrotex JSC/
Tel: +7 4862 440642;

Direct Bonded Copper (DPC Substrates)

www.curamik.co.uk
curamik® electronics GmbH
Tel: +49 9645 9222 0

Discrete Semiconductors

www.digikey.com/europe
Digi-Key
Tel: +31 (0)53 484 9584

www.microsemi.com
Microsemi
Tel: 001 541 382 8028

Drivers ICS

www.power.ti.com
Texas Instruments
Tel: +44 (0)1604 663399

EMC/EMI

www.dextermag.com
Dexter Magnetic Technologies, Inc.
Tel: 001 847 956 1140

Ferrites & Accessories

www.dextermag.com
Dexter Magnetic Technologies, Inc.
Tel: 001 847 956 1140

GTO/Triacs

www.mark5.com
Mark 5 Ltd
Tel: +44 (0)2392 618616

Hall Current Sensors

www.dgseals.com
dgseals.com
Tel: 001 972 931 8463

Harmonic Filters

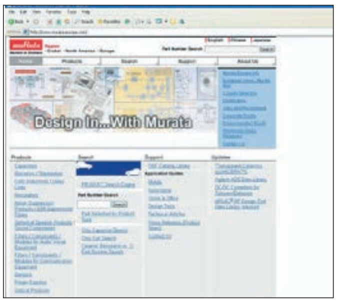

www.murata-europe.com
Murata Electronics (UK) Ltd
Tel: +44 (0)1252 811666

High Voltage and High Power Electronics

Dean Technology, Inc.
www.deantechnology.com
+1 (972) 248-7691

IGBTs

www.microsemi.com
Microsemi Tel: 001 541 382 8028

www.power.ti.com
Texas Instruments
Tel: +44 (0)1604 663399

Line Simulation
www.hero-power.com
Rohrer GmbH
Tel.: +49 (0)89 8970120

Magnetic Materials/Products
www.dextermag.com
Dexter Magnetic Technologies, Inc.
Tel: 001 847 956 1140

Mosfets
www.aosmd.com
Alpha and Omega Semiconductor
Tel: 001 408 789 3233

www.mark5.com
Mark 5 Ltd
Tel: +44 (0)2392 618616

www.microsemi.com
Microsemi
Tel: 001 541 382 8028

www.neutronltd.co.uk
Neutron Ltd
Tel: +44 (0)1460 242200

Optoelectronic Devices
www.digikey.com/europe
Digi-Key Tel: +31 (0)53 484 9584

www.power.ti.com
Texas Instruments
Tel: +44 (0)1604 663399

Packaging & Packaging Materials
www.curamik.co.uk
curamik® electronics GmbH
Tel: +49 9645 9222 0

Power Amplifiers
www.rohrer-muenchen.de
Rohrer GmbH
Tel: +49 (0)89 8970120

Power ICs
www.digikey.com/europe
Digi-Key Tel: +31 (0)53 484 9584

www.power.ti.com
Texas Instruments
Tel: +44 (0)1604 663399

Power Modules
www.picoelectronics.com
Pico Electronics
Tel: +44 1634 298900

www.psl-group.uk.com
PSL Group UK Ltd.
Tel +44 (0) 1582 676800

www.fujielectric-europe.com
Fuji Electric Europe GmbH
Tel: +49 (0)69-66902920

www.microsemi.com
Microsemi Tel: 001 541 382 8028

www.proton-electrotex.com/
Proton-Electrotex JSC/
Tel: +7 4862 440642;

Power Protection Products
www.power.ti.com
Texas Instruments
Tel: +44 (0)1604 663399

Power Semiconductors
www.psl-group.uk.com
PSL Group UK Ltd.
Tel +44 (0) 1582 676800

www.proton-electrotex.com/
Proton-Electrotex JSC/
Tel: +7 4862 440642;

Power Substrates
www.universal-science.com
Universal Science Ltd
Tel: +44 (0)1908 222211

Resistors & Potentiometers
www.isabellenhuette.de
Isabellenhütte Heusler GmbH KG
Tel: +49/(27 71) 9 34 2 82

RF & Microwave Test Equipment.
www.ar-europe.ie
AR Europe
Tel: 353-61-504300

Simulation Software
www.power.ti.com
Texas Instruments
Tel: +44 (0)1604 663399

www.universal-science.com
Universal Science Ltd
Tel: +44 (0)1908 222211

Smartpower Devices
www.irf.com
International Rectifier Co. (GB) Ltd
Tel: +44 (0)1737 227200

Solder
www.indium.com
Indium Corporation
Tel: +44 (0) 1908-580400

Switched Mode Power Supplies
www.citapower.com
Bias Power, LLC
Tel: 001 847.419.9118

www.power.ti.com
Texas Instruments
Tel: +44 (0)1604 663399

Thermal Management & Heatsinks
www.universal-science.com
Universal Science Ltd
Tel: +44 (0)1908 222211

Thermal Management & Heatsinks
www.psl-group.uk.com
PSL Group UK Ltd.
Tel +44 (0) 1582 676800

Thermal Management & Heatsinks
www.abl-heatsinks.co.uk
ABL Components Ltd
Tel: +44 (0) 121 789 8686

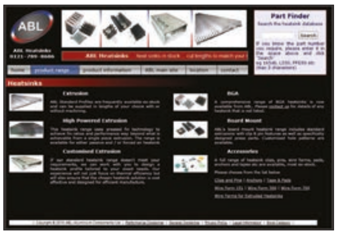

www.curamik.co.uk
curamik® electronics GmbH
Tel: +49 9645 9222 0

www.dau-at.com
Dau GmbH & Co KG
Tel: +43 3143 23510

www.power.ti.com
Texas Instruments
Tel: +44 (0)1604 663399

Thyristors
www.mark5.com
Mark 5 Ltd
Tel: +44 (0)2392 618616

www.proton-electrotex.com/
Proton-Electrotex JSC/
Tel: +7 4862 440642;

ADVERTISERS INDEX